

**Synthesis of Carbon Nanotubes (CNTs) as
Thermal Interface Material**

by

Baha Yakupoglu

A thesis submitted to the Graduate Faculty of
Auburn University
in partial fulfillment of the
requirements for the Degree of
Master of Science

Auburn, Alabama
December 14, 2013

Keywords: Carbon nanotubes, CNT, Chemical Vapor Deposition, CVD,
Sputtering Growth time

Copyright 2013 by Baha Yakupoglu

Approved by

Hulya Kirkici, Chair, Professor of Electrical and Computer Engineering
Thomas Baginski, Professor of Electrical and Computer Engineering
Bogdan Wilamowski, Professor of Electrical and Computer Engineering

Abstract

Carbon nanotubes (CNTs) are promising materials for many potential applications. High electrical conductivity, superior mechanical strength, thermal conductivity, and chemical inertness are some of the properties of CNTs. CNTs can carry high – current densities, and they have been studied as cold – cathode field emitters. Small diameter and relatively long length of CNTs makes them perfect field emitters with high emission currents at low electric fields.

In this thesis, electrical and thermal properties of CNTs considered. For this, selective and non – selective multi – wall carbon nanotubes (MWCNTs) are synthesized by Chemical Vapor Deposition (CVD) method. CNTs are synthesized on both Nickel (Ni) and Silicon (Si) substrates. In some cases, SiO₂ under layer is employed on silicon wafer. Iron (Fe), Nickel (Ni), and Carbon (C) are used as catalyst types onto Si and SiO₂ coated Si substrates. The SEM images, growth conditions and their effects such as catalyst thicknesses, DC/RF sputtering distance, sputtering pressure, gas flow rate, and CVD temperature effects are discussed. The patterned CNT fabrication process is also studied in this thesis.

Acknowledgments

It gives me a great pleasure in acknowledging the support and help of Professor Hulya Kirkici, who was not only an advisor, but also a motherly figure to me during this research. I would have not completed this study without her motivation, love, encouragement, guidance, suggestions, and valuable comments. It is a distinguishing opportunity to feel her support all the time for my professional development.

I also would like to express my many and sincere thanks to Professor Thomas Baginski, and Professor Bogdan Dan M. Wilamowski for their time and effort to review my thesis and being a part of my committee. It was also a great pleasure to be a part of their classes.

My thanks also go to all our lab mates and all research group members for establishing a fun environment during this research period. Special thanks to Roger Tsai, Huirong Li, Rujun Bai, and Ming Zhang for all their support.

Most of all, I'd like to thank my parents, Suheyla and Cevat Yakupoglu, and my uncle Semih Ozkurtaran for all their lifetime support, love, encouragement, and dedication.

Finally, I'd like to thank my wife, Funda Yakupoglu. She was always here to cheer me up and stood by me through the good and bad.

*To the memory of my mom
who loved me with all her heart*

Table of Contents

Abstract	ii
Acknowledgments	iii
List of Tables	vii
List of Figures	viii
Chapter 1 Introduction	1
Chapter 2 Literature Review	5
2.1 Carbon Nanotube Structures	5
2.2 Carbon Nanotube Properties	7
2.2.1 Electrical Properties	8
2.2.2 Mechanical Properties	9
2.2.3 Chemical Properties	10
2.3 Carbon Nanotube Synthesis Techniques	11
2.4 CVD, thermal CVD, and PECVD	15
Chapter 3 Carbon Nanotubes Fabrication and Characterization	19
3.1 Overview	19
3.2 Wafer Cleaning and Catalyst Deposition	20
3.3 Patterning and Masking Process	22
3.4 Nickel as a Substrate to Grow CNTs	24
3.5 CNT Growth Process in CVD	25

Chapter 4 Results and Discussion.....	27
4.1 Catalyst Thickness Effect	27
4.2 DC/RF Sputtering Distance and Pressure Effect	30
4.3 Flow Rate Effect	31
4.4 CVD Temperature Effect.....	31
4.5 SEM Images (Collection)	32
Chapter 5 Conclusions	40
References	41

List of Tables

Table 2.1	Young's modulus, tensile strength, and density of CNTs compared with the other materials	10
Table 4.1	Varying layer thicknesses depending on the sputtering pressure	31

List of Figures

Figure 1.1	Atomic structure of carbon nanotubes a) Graphite lattice b) Single – walled CNT c) Multi – Walled CNT	2
Figure 1.2	a) arc – discharge MWCNT TEM image b) CVD MWCNT TEM image c) arc – discharge MWCNT AFM image d) CVD MWCNT AFM image	3
Figure 2.1	sp^2 hybridization of carbon and its derived materials a) The three sp^2 hybridized orbital are in-plane, with 2p orbital orthogonal to the plane, π and π^* denotes the bonding and anti – bonding orbital b) Graphene as the source of three different materials, fullerene (left), carbon nanotube (center) and bulk graphite (right).....	5
Figure 2.2	a) A two – dimensional honeycomb lattice two show different types of tubules can be formed, and defined by chiral vectors b) An example of (4,2) CNT construction.....	7
Figure 2.3	Raman spectroscopy of 8 mins Carbon (C) sputtered on already 5 mins Fe sputtered Si substrate after CVD growth using ion laser excitation of a) 514 nm visible and b) 785 nm near infrared wavelengths (CVD growth conditions were 700 ⁰ C, 70.8 mTorr, and the Ar : C ₂ H ₂ rate was 75sccm : 20sccm)	9
Figure 2.4	Currently used methods for Carbon Nanotubes Synthesis	12
Figure 2.5	Schematics of the arc-discharge apparatus employed for fullerene and nanotube production (b) image of the arc experiment between two graphite rods (courtesy of P. Redlich). The extreme temperature reached during the experiment is located between the rods (~3000–4000 K).....	13
Figure 2.6	Schematic of Laser Ablation method	14
Figure 2.7	Thermal CVD schematic diagram to growth CNTs.....	16
Figure 2.8	Plasma enhanced CVD schematic diagram to growth CNTs.....	17
Figure 3.1	Schematic and picture of DC/RF Sputtering Chamber, Plasma gun, and substrate holder.....	21
Figure 3.2	x2000 and x7000 SEM images of 5 minutes iron (Fe) sputtered Silicon substrate surface.....	21

Figure 3.3	The patterned Si substrate by 0.5 cm ² holes after the development step.	22
Figure 3.4	a) CNTs on Si substrate by 0.5 cm ² holes after 5 minutes Fe sputtering and 20 minutes CVD growth. b) CNTs on Si substrate by 0.5 cm ² holes after 5 minutes Fe sputtering and 20 minutes CVD growth. (Growth conditions were 700 ⁰ C, 70.8 mTorr, and the Ar : C ₂ H ₂ rate was 75sccm : 20sccm).....	23
Figure 3.5	Illustrated flow chart of patterned CNT synthesis. a) Positive – tone photoresist step. b) Mask alignment step. c) Dry and wet etching. d) 5 minutes Fe sputtering. e) Removing the PR. f) CVD growth.....	24
Figure 3.6	Fe catalyst sputtered for 5 minutes on Ni Foil (resolution x20k).....	25
Figure 3.7	A schematic diagram of the thermal CVD system.....	26
Figure 4.1	a) 10 nm deposition thickness of Fe results with very dense CNTs on Si substrate. b) >10 nm deposition thickness of Ni results with very dense CNTs on Si substrate. (Both pictures are taken after 20 minutes CVD growth. Growth conditions were 700 ⁰ C, 70.8 mTorr, and the Ar : C ₂ H ₂ rate was 75sccm : 20sccm.).....	27
Figure 4.2	8 minutes C sputtering on already 5 minutes Fe sputtered Si substrate. (Picture is taken after 20 minutes CVD growth. Growth conditions were 700 ⁰ C, 70.8 mTorr, and the Ar : C ₂ H ₂ rate was 75sccm : 20sccm.).....	28
Figure 4.3	a) Ni 5 minutes, and Fe 5 minutes sputtering on SiO ₂ b) Pretreated Ni 5 minutes, and Fe 5 minutes sputtering on SiO ₂ c) Ni 7 minutes sputtering, 8 hours annealing, and Fe 5 minutes sputtering respectively on SiO ₂ (Both pictures are taken after 20 minutes CVD growth. Growth conditions were 700 ⁰ C, 70.8 mTorr, and the Ar : C ₂ H ₂ rate was 75sccm : 20sccm.)	29
Figure 4.4	Left side of the substrate respect to the Fig 3b -Ni 5 minutes, and Fe 5 minutes sputtered SiO ₂ sample (Picture is taken after 20 minutes CVD growth. Growth conditions were 700 ⁰ C, 70.8 mTorr, and the Ar : C ₂ H ₂ rate was 75sccm : 20sccm.)	30
Figure 4.5	Randomly oriented CNTs grown of Fe catalyst sputtered for 5 minutes on Si substrate (resolution x10k)	33
Figure 4.6	Randomly oriented CNTs grown of Fe catalyst sputtered for 1 minute on SiO ₂ substrate (resolution x10k).....	33
Figure 4.7	Randomly oriented CNTs grown of Fe catalyst sputtered for 5 minutes on SiO ₂ substrate (resolution x10k).....	34

Figure 4.8	Ni catalyst sputtered for 5 minutes on Si substrate (resolution x50k).....	34
Figure 4.9	Ni catalyst sputtered for 5 minutes on top of the Fe catalyst sputtered for 5 minutes Si substrate (resolution x30k)	35
Figure 4.10	Cross – sectional image of Ni catalyst sputtered for 3 minutes on top of the Fe catalyst sputtered for 5 minutes Si substrate (resolution x20k)	35
Figure 4.11	Ni catalyst for 3 minutes, Fe catalyst for 5 minutes, and C catalyst for 8 minutes sputtered on Si substrate (resolution x30k).....	36
Figure 4.12	Cross – sectional image of C catalyst sputtered for 8 minutes on top of the Fe catalyst sputtered for 5 minutes Si substrate (resolution x10k)	36
Figure 4.13	Fe catalyst sputtered for 5 minutes on Ni Foil (resolution x20k).....	37
Figure 4.14	Ni catalyst sputtered for 5 minutes on top of the Fe catalyst sputtered for 5 minutes SiO ₂ substrate (resolution x10k).....	37
Figure 4.15	Ni catalyst sputtered for 7 minutes on top of the Fe catalyst sputtered for 5 minutes SiO ₂ substrate (resolution x20k)	38
Figure 4.16	Ni catalyst sputtered for 10 minutes on top of the Fe catalyst sputtered for 5 minutes SiO ₂ substrate (resolution x20k).....	38
Figure 4.17	Side image of Fe catalyst sputtered for 5 minutes on .5 cm ² x .5 cm ² patterned Si substrate (resolution x10k).....	39
Figure 4.18	Cross – sectional image of Fe catalyst sputtered for 5 minutes on .35 cm ² x .35cm ² patterned Si substrate (resolution x10k).....	39

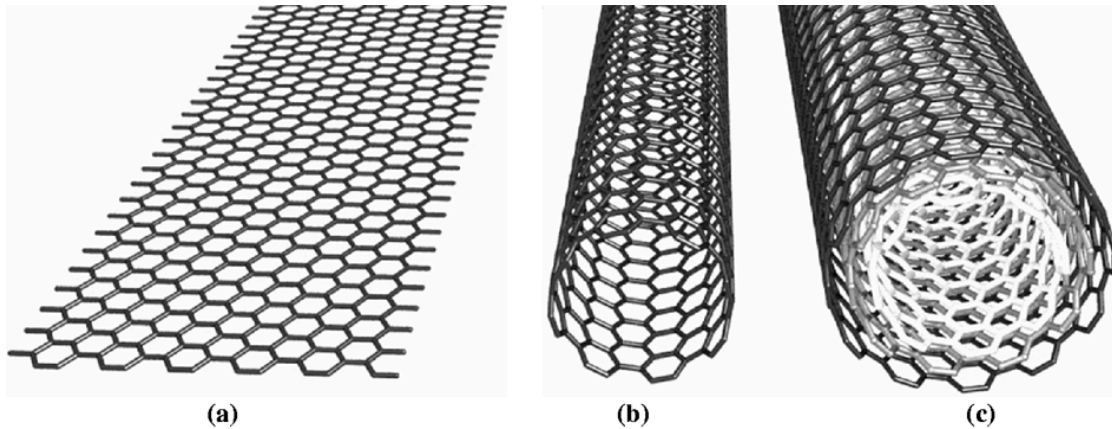
Chapter 1

Introduction

Carbon nanotubes (CNTs) are a kind of macromolecule of carbon, which can be thought of as graphitic sheets with a hexagonal lattice that are rolled into a smoothly continuous cylinder. Due to their exceptional electrical, mechanical, and chemical properties, CNTs have motivated a wide area of research, since their first discovery in 1990s, in both science, and engineering on their fabrications, and applications [1]. CNTs have many structures depending on thicknesses, lengths, number of layers and the type of helicities. They are classified according to these structures, and their electrical characteristics rely on these categories. Their structure is typically categorized as single – wall carbon nanotubes (SWCNTs), and multi – wall carbon nanotubes (MWCNTs) with respect to the graphitic layers as illustrated in Figure 1.1 [2]. The simplest MWCNT is called double – wall CNT (DWCNT), which is formed only from two layers. Moreover, the dissymmetry (wrapping angle) of the configuration of the CNTs is taken into consideration and affects their density, lattice structure, conductivity, and whether they act as metals or as semiconductors. I'll describe these forms by chiral vectors in chapter 2.

The strength and the remarkable physical properties of CNTs like persistency, stiffness...etc. can be unfurled by finding the correct form. In fact, they can be up to a hundred times stronger than steel, while 6 times lighter than it [3]. These special properties open a wide range of aspects to CNTs as practical and commercial products at new, and existing applications such as field effect / single – electron transistors [4 – 8], conductive plastics, biosensors [9], structural composite materials, radar – absorbing

coating, atomic force microscope (AFM) tips [10], batteries with improved lifetime, ultra capacitors, extra strong fibers, and field emitters [11].



Source: Kreupl *et al.* (2004)

Figure 1.1 Atomic structure of carbon nanotubes a) Graphite lattice b) Single – walled CNT c) Multi – Walled CNT [2]

Nanotubes have very impressive electric field emission properties, and they are extremely conductive. Their turn – on voltage can be as low as 1 – 3 V/ μm , and emission current could be up to 0.1 mA [12]. Thus, they are also a promising material in high current density applications, and lightweight packaging as a cold – cathode field emission source. In addition, they can carry very large (up to 100 MA/ cm^2 [13]) current densities, and they sustain this superconductivity, even with the transition of temperatures up to 5 K [14]. They have thermal conductivity up to 3000 W/m K [15].

There are a couple of well – known techniques that are used to synthesize CNTs including arc – discharge, laser ablation, and chemical vapor deposition (CVD). Arc – discharge and laser ablation are the first used methods to produce CNTs. These methods produce relatively less defective CNTs in comparison to the other techniques. However, CVD method is more preferable and popular nowadays, due to relatively cheap and easy

production of very large quantities of CNTs. Unfortunately, the CVD technique presents large quantities of defects, and CNTs' chemical, electrical, and mechanical properties suffer from these defects. Yet, above advantages, plus easy control of the reaction course, and high purity of the obtained material [16] make this technique the most suitable one for a potential industrial level production. Transmission electron microscope (TEM) and atomic force microscope (AFM) pictures of arc – discharge MWCNTs, and CVD MWCNTs as shown in Figure 1.2 [17].

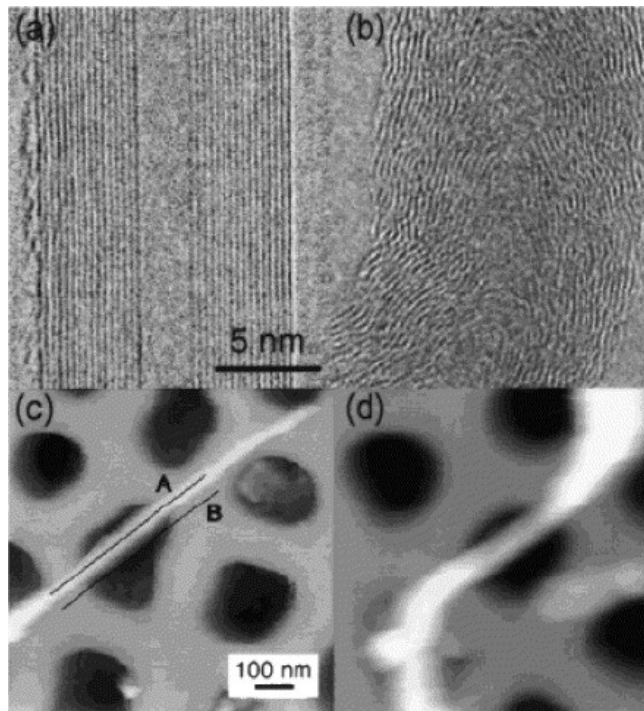


Figure 1.2 a) arc – discharge MWCNT TEM image b) CVD MWCNT TEM image
c) arc – discharge MWCNT AFM image d) CVD MWCNT AFM image [37]

Randomly aligned carbon nanotubes were synthesized and were studied by using chemical vapor deposition technique in this thesis. Iron (Fe), Nickel (Ni), and Carbon (C) are used as catalysts. Growth conditions, catalyst thickness effect, DC / RF sputtering

distance and pressure effect, flow rate effect, and CVD temperature effect are investigated. Furthermore, using photolithography steps, different sizes (0.5 cm^2 by 0.5 cm^2 , and 0.35 cm^2 by 0.35 cm^2) of patterned CNTs are also successfully synthesized.

Chapter 2

2.1 Carbon Nanotube Structures

Carbon is an active element to produce different molecular compounds and crystallized solids. Fullerene, CNT, and graphite are a couple of examples of carbon – bonded materials that have unique nanometer sizes of sp^2 forms as seen in Figure 2.1 [20]

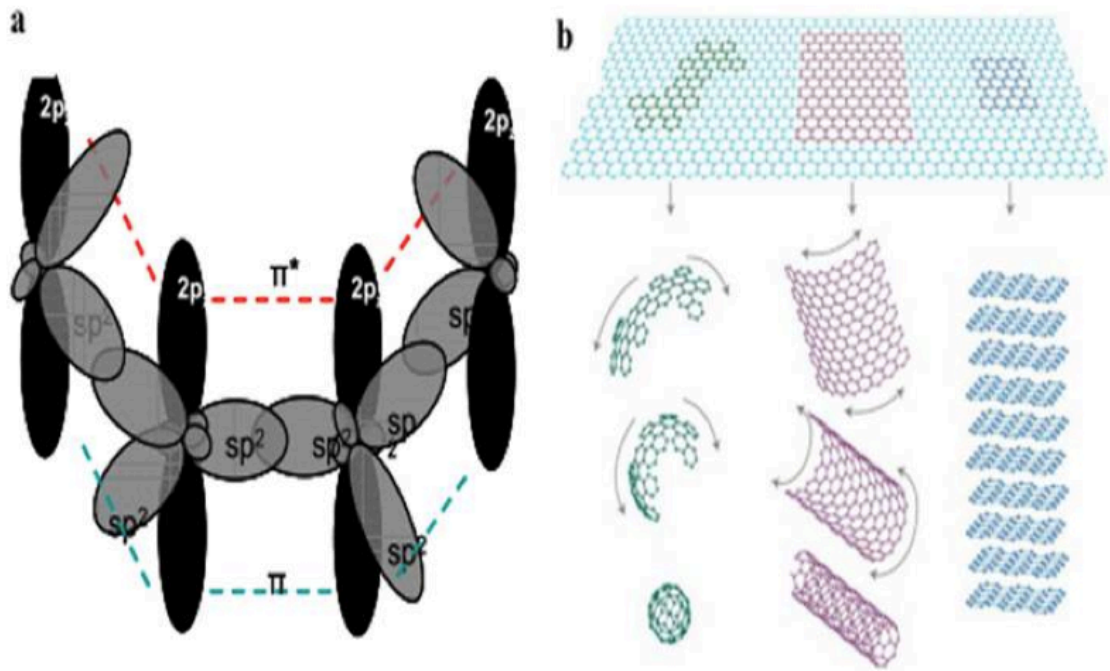


Figure 2.1 sp^2 hybridization of carbon and its derived materials a) The three sp^2 hybridized orbital are in-plane, with $2p$ orbital orthogonal to the plane, π and π^* denotes the bonding and anti – bonding orbital b) Graphene as the source of three different materials, fullerene (left), carbon nanotube (center) and bulk graphite (right) [20]

CNT structures are determined by the wrapping angle of the hexagonal graphene sheets. Chiral vectors can describe these forms. They can be either “arm – chair”, “zig –

zag” or several non – standard chiral structures. The chiral vector equation can be described as $\vec{R} = n\vec{a}_1 + m\vec{a}_2$ (where the n, and m are integers), and can be explained easily with Figure 2.2a. The condition for the chirality convention should be $n \geq |m| \geq 0$. We begin with describing the tube axis by drawing two lines (the green lines). Then, we arbitrarily choose a point on one of the lines and call it A. Then, we draw our armchair line (yellow line) between two tube axis lines, which separates the honeycombs to two equal halves. After we draw the armchair line, we choose another point on the tube axis line that corresponds to a carbon atom, and also is closest to the armchair line, and call it B. The red line, which connects these two points, will be our chiral vector R. The angle between the chiral vector R, and the armchair line is called the wrapping angle, ϕ . If the chiral vector R is on the armchair line, in other words if the wrapping angle $\phi=0^\circ$, the tube is called “armchair”. If the wrapping angle $\phi=30^\circ$, the tube is called “zig – zag”. Lastly, for $0^\circ < \phi < 30^\circ$, it is called chiral tube. The values of the n, and m influence the chirality of the tube, which affect the conductivity, density etc. of the CNTs.

The diameter of the tube can be described using the relationship:

$$d = \frac{|\vec{R}|}{\pi} = \frac{a\sqrt{m^2 + mn + n^2}}{\pi}$$

and the wrapping angle can be described as:

$$\cos\phi = \frac{|\vec{R} \cdot \vec{a}_1|}{|\vec{R}||\vec{a}_1|} = \frac{2n + m}{2\sqrt{m^2 + mn + n^2}}$$

When the difference n-m is divisible by three, the SWCNT is considered to be a metallic nanotube. Otherwise, it is considered to be a semiconducting one. In most of the cases, while the n, and m are random numbers, the formed nanotubes can be expected to be 2/3 is semiconducting, and the final third metallic. [21]

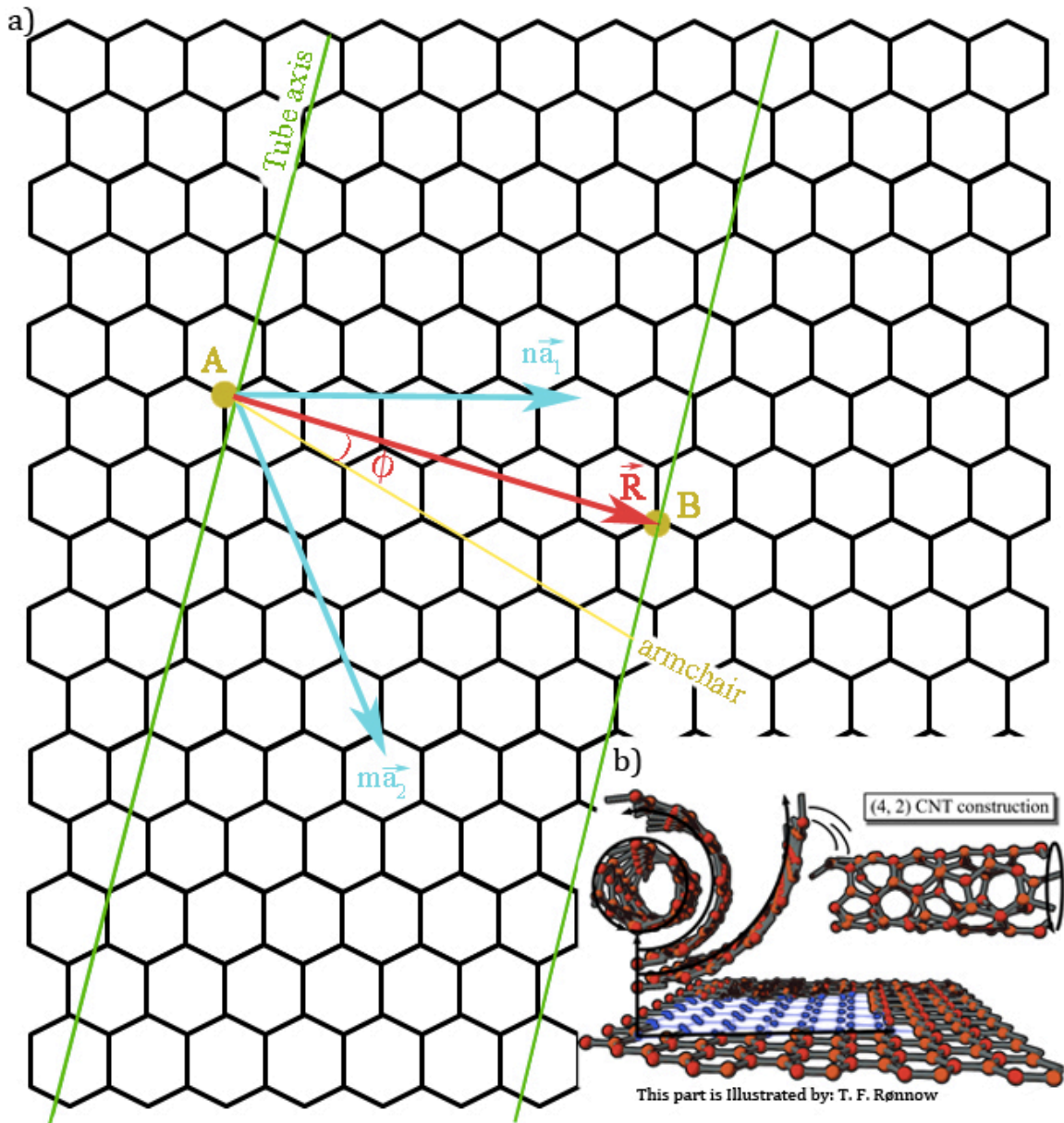


Figure 2.2 a) A two – dimensional honeycomb lattice two show different types of tubules can be formed, and defined by chiral vectors b) An example of (4,2) CNT construction

2.2 Carbon Nanotube Properties

Three properties of CNTs, which are electrical, chemical, and mechanical, are the most important and widely researched for the manufacturing and the application purposes.

2.2.1 Electrical Properties

The properties of CNTs show excellent features such as conductivity, and resistivity. There are a couple of different techniques that are in use to determine these properties. Some of the common – use of them are Raman spectroscopy [22], four – point probe technique [23], electron spin resonance (ESR) [24], scanning tunneling microscopy (STM) [25], atomic force microscopy (AFM), and electron energy loss spectroscopy (EELS) [26]. Figure 2.3 shows a CNT structure that was studied under Raman spectroscopy using ion laser excitation of both 514 nm visible and 785 nm near infrared wavelengths. Those samples were fabricated in – house by CVD method.

Ebbesen et al. [23] measured the resistivities of MWCNTs by using the four – point probe technique where the tungsten wires used as probes. The results are ranged between $5.1 \times 10^{-6} \Omega - \text{cm}$ to $1.2 \times 10^{-4} \Omega - \text{cm}$. The resistivities of SWCNTs are also measured by using the same technique by Smalley et al. [27]. The results range from $0.34 \mu\Omega - \text{m}$ to $1 \mu\Omega - \text{m}$. Moreover, CNTs can carry up to 100 MA/cm^2 current densities [28], and high thermal conductivity of $\sim 200 \text{ W/m K}$ has been measured by Benes et al. [29].

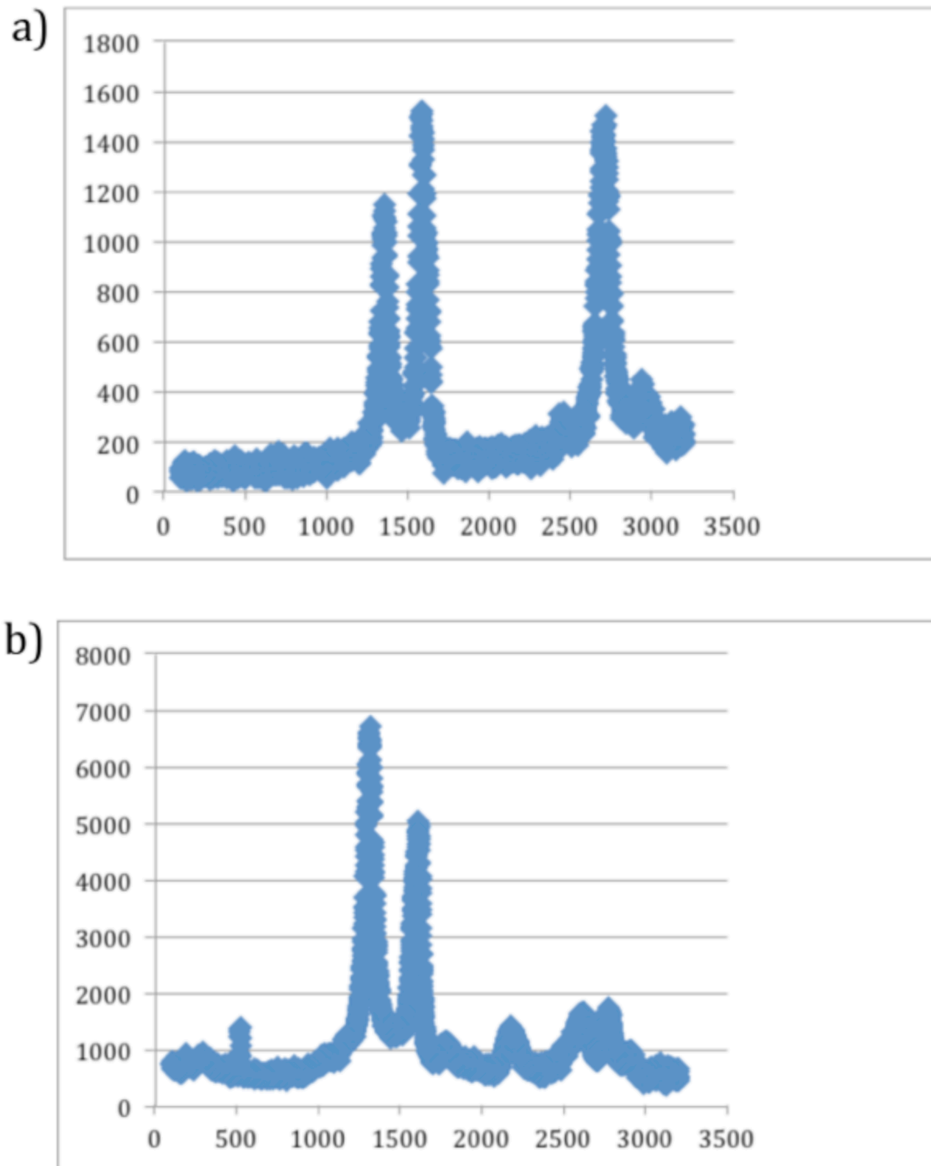


Figure 2.3 Raman spectroscopy of 8 mins Carbon (C) sputtered on already 5 mins Fe sputtered Si substrate after CVD growth using ion laser excitation of a) 514 nm visible and b) 785 nm near infrared wavelengths (CVD growth conditions were 700⁰C, 70.8 mTorr, and the Ar : C₂H₂ rate was 75sccm : 20sccm)

2.2.2 Mechanical Properties

The CNTs are very strong materials. They have great stiffness and tensile strength. Lots of measurements have been made to calculate the Young's modulus, and the strength of CNTs [30], [31]. Furthermore, the comparison of these calculations with

the other materials has been shown [32]. Table 2.1 shows The Young's modulus, tensile strength and densities of SWCNTs and MWCNTs compared with the other materials. The average Young's modulus of CNTs is around 1.8 TPa, which is a high value considering that the maximum value of the Young's modulus of the steel is .186 TPa. Since MWCNTs are formed from multiple layers of SWCNTs, and the highest value of Young's modulus of SWCNTs are calculated depending on the coaxial intertube coupling of Van der Walls Force [33], the modulus value is higher for the MWCNTs.

Material	Young's modulus(GPa)	Tensile Strength(GPa)	Density(g/cm ³)
MWNT	1200	150	2.6
Single-wall nanotube	1054	150	1.3
SWNT bundle	563	150	1.3
Graphite (in plane)	350	2.5	2.6
Steel	208	0.4	7.8
Epoxy	3.5	0.005	1.25
Wood	16	0.008	0.6

Table 2.1 Young's modulus, tensile strength, and density of CNTs compared with the other materials [32]

2.2.3 Chemical Properties

Although CNTs show low chemical reactivity, oxidation is an important chemical reaction, which is effective on CNTs at high temperatures over 750°C. The oxidation begins from the tips of the CNTs, and goes inwards layer by layer at the MWCNTs. Since it begins from the tips and affects the layers, it is possible to have open and thinner CNTs

after this reaction. This process can be resulted with different oxides groups [34] that enhance CNTs chemical reactivity and change their wetting, opening etc. properties.

Some promising applications that exist because of the chemical properties of CNTs such as absorbing molecules with non – covalent forces are cancer therapy, and drug delivery [35], and [36]. Biosensors are another important area that CNTs can be used to fabricate ultrasensitive levels. Shibayama et al. reported a glucose biosensor with a sensitivity of $40\mu\text{A mM}^{-1}\text{ cm}^{-2}$, a correlation coefficient of .992, a linear response range of .025 – 1.9 mM, a detection limit of 6.2 μM at $S/N=3$, +.8 V vs Ag/AgCl [37]. These ultrasensitive biosensors can also be used in DNA detection [38].

Furthermore, CNTs can be fabricated as the darkest material, which makes them a perfect candidate for the future solar – cell applications.

2.3 CNT Synthesis Techniques

The first methods to growth CNTs were arc – discharge and laser ablation ones. Nowadays, these processes yield their place to Chemical Vapor Deposition (CVD) technique. CVD method is useful for both controlling CNTs orientation and length, and also for allowing large area processing relatively cheaply. There are also a couple of assisted approaches to CVD method such as thermal chemical vapor deposition, plasma enhanced chemical vapor deposition (PECVD), radio frequency chemical vapor deposition (RF – CVD), microwave plasma enhanced chemical vapor deposition (MPECVD), hot filament chemical vapor deposition, water – assisted chemical vapor deposition, and oxygen – assisted chemical vapor deposition as shown in Figure 2.4 [19].



Figure 2.4 Currently used methods for Carbon Nanotubes Synthesis [19]

Arc discharge and laser ablation methods occur at high temperatures. Synthesized CNTs with these techniques usually have fewer defects compared with CVD technique. Both techniques condense carbon atoms from evaporation of solid carbon sources onto substrates. Inert gases like helium or argon are usually introduced in arc – discharge technique, and CNTs are formed through arc – vaporization of two-graphite rods placed end to end that act as anodes and cathodes. They are separated by about 1 mm at low pressure. The important factors that affect the type, and quality of the formed CNTs are gas pressure, plasma uniformity, and deposit temperature formed on the electrode with this technique. An arc – discharge apparatus schematic, and an experiment picture are shown in Figure 2.5 [39]

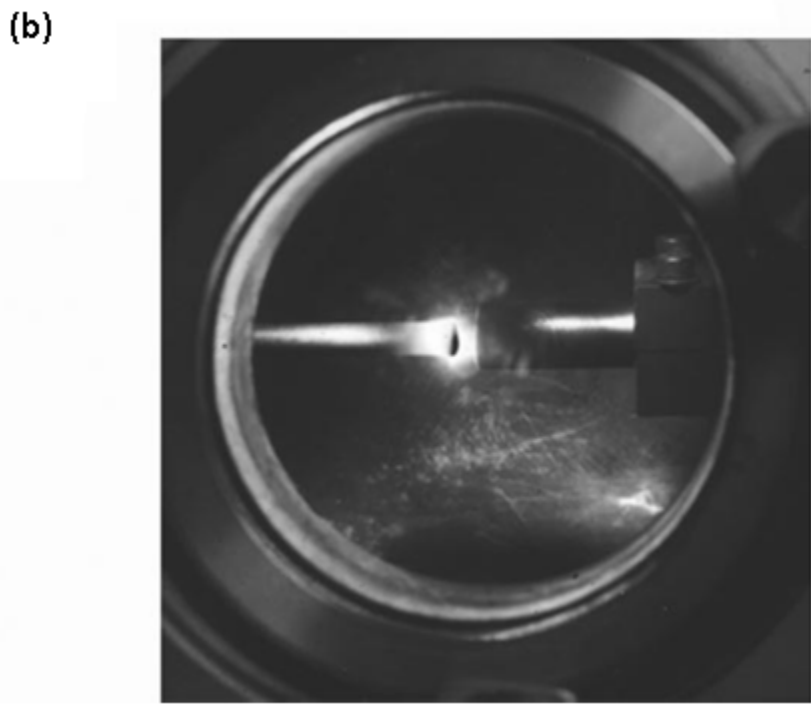
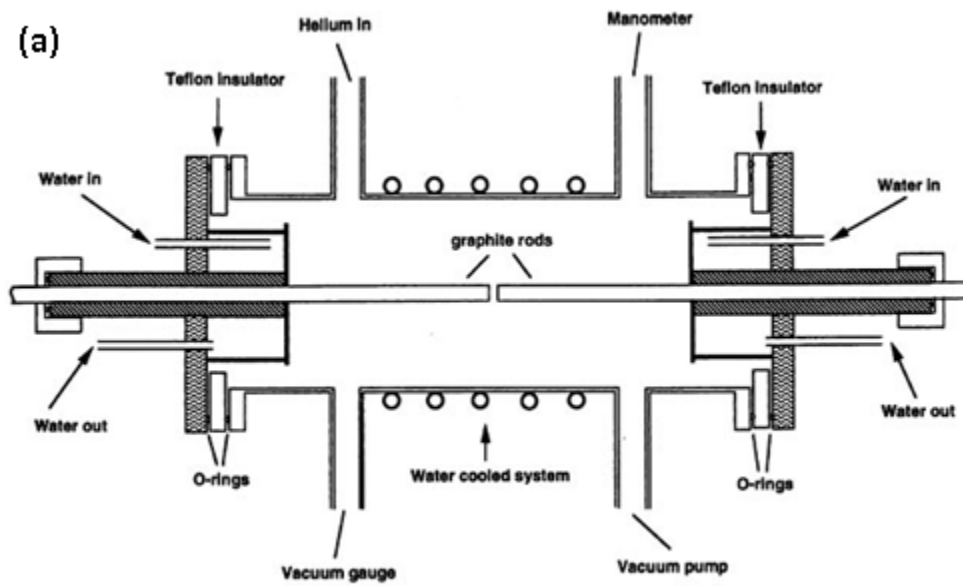


Figure 2.5 (a) Schematics of the arc-discharge apparatus employed for fullerene and nanotube production (b) image of the arc experiment between two graphite rods (courtesy of P. Redlich). The extreme temperature reached during the experiment is located between the rods ($\sim 3000\text{--}4000\text{ K}$) [39]

Laser ablation is one of the other good methods to synthesize high quality and pure CNTs. It is first used by Smalley et al. [40]. As in arc – discharge method, there are lots of critical parameters that affect the formed tubes such as laser properties, inert gas pressure, temperature, and target material structure. [19] The basic mechanism and principle of this method is carbon target vaporization as in arc – discharge technique. The difference is that the laser provides the energy that hits the graphite target, which is located in the oven, and contains catalyst materials mostly nickel (Ni) or Cobalt (Co). The synthesized CNTs pass the chamber with the help of the inert gas flow, and are collected on a cold finger. A schematic of this method is shown in Figure 2.6.

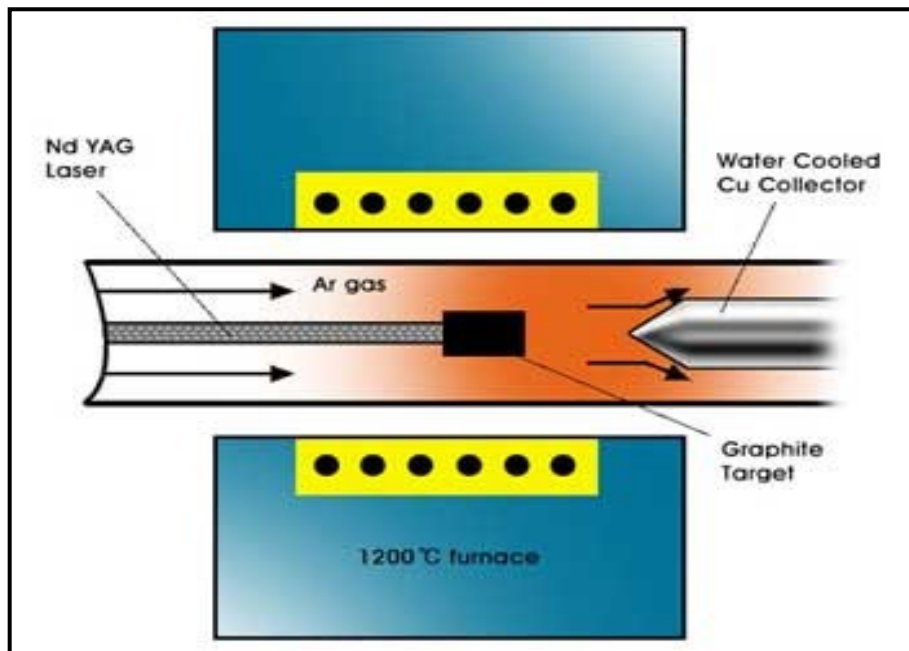


Figure 2.6 Schematic of Laser Ablation method [41]

2.4 CVD, Thermal CVD, and PECVD

Chemical vapor deposition method is the most common, and relatively economic technique so far that is used to grow CNTs. Although the CNTs synthesized by this technique suffer from very large quantities of defects, economic reasons, simplicity, controllable growth, and mass production capabilities give a priority to this method.

Catalyst preparation, and actual growth are two important steps in CVD method. The preparation of the catalyst involves sputtering of transition metals like iron (Fe), and nickel (Ni) on to the substrate materials as it is studied in this thesis. Also, gaseous phase activated carbon is required for actual growth. It is common to use gaseous carbon sources such as acetylene, methane, and carbon monoxide (CO), and we can classify the methods in use to activate these molecules as plasma enhanced CVD and thermal CVD [42]. Thermal CVD uses conventional heat sources to heat the furnace to the desired temperature such as infrared lamp, resistive, or inductive filaments. Since the catalyst has an influential effect on both growth rate and produced CNTs [43], different techniques are studied at the preparation level of catalyst such as metallic alloys. For instance, Cobalt (Co), and Fe alloy gives 10 – 100 times more SWCNTs than pure iron [44]. The catalyst dimensions also affect the CNT production. While the large particles can be useful to synthesize MWCNTs, dimensions that are too large can result in carbon fibers or filaments [42]. Moreover, metal particle concentration, and deposition temperature have effects on CNTs growth too [45]. A schematic illustration of thermal CVD can be seen in Figure 2.7.

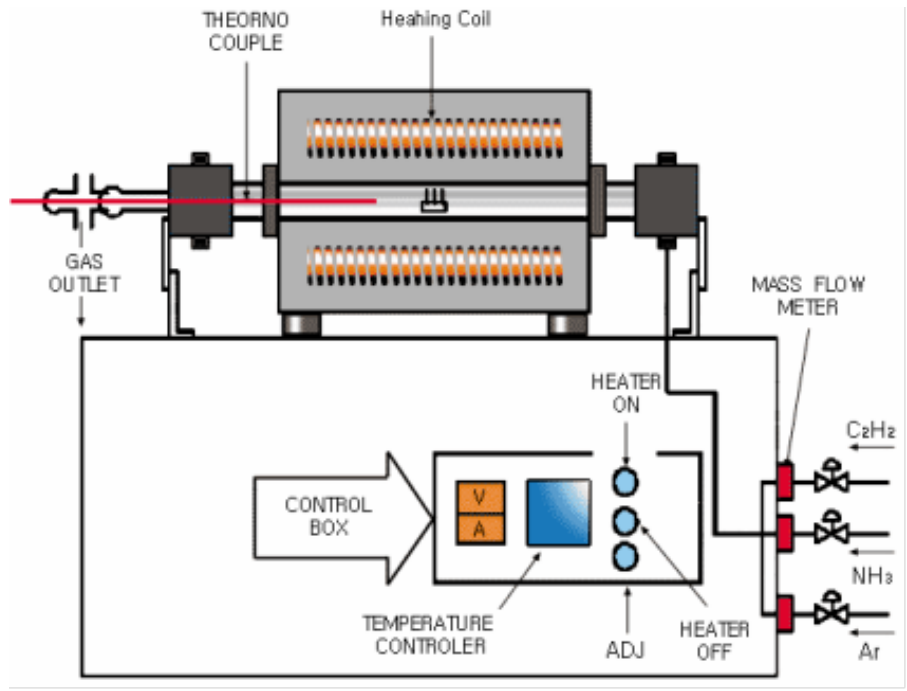


Figure 2.7 Thermal CVD schematic diagram to growth CNTs [41]

In the plasma enhanced CVD method, high voltage and high frequency are applied to both electrodes, and CNTs are synthesized in a furnace by glow discharge. Plasma has been used as an activator and decomposer of the reactants in the gas phase, and a source to generate glow discharge in PECVD technique. Electrical discharges at DC, RF, and MW frequencies, and hot – filament are mostly used to generate the plasma. There are two parallel plate electrodes located in the PECVD chamber, and the substrate is placed on the grounded electrode. It is important to keep the $p \times d$ equation constant (where d is the distance between the electrodes, and p is the pressure of the chamber) to be able to maintain the discharge. It is important to have the desired substrate temperature stabled in order to increase the nucleation density. A separate heater might be used for that reason. A schematic of the PECVD can be seen in Figure 2.8 [46].

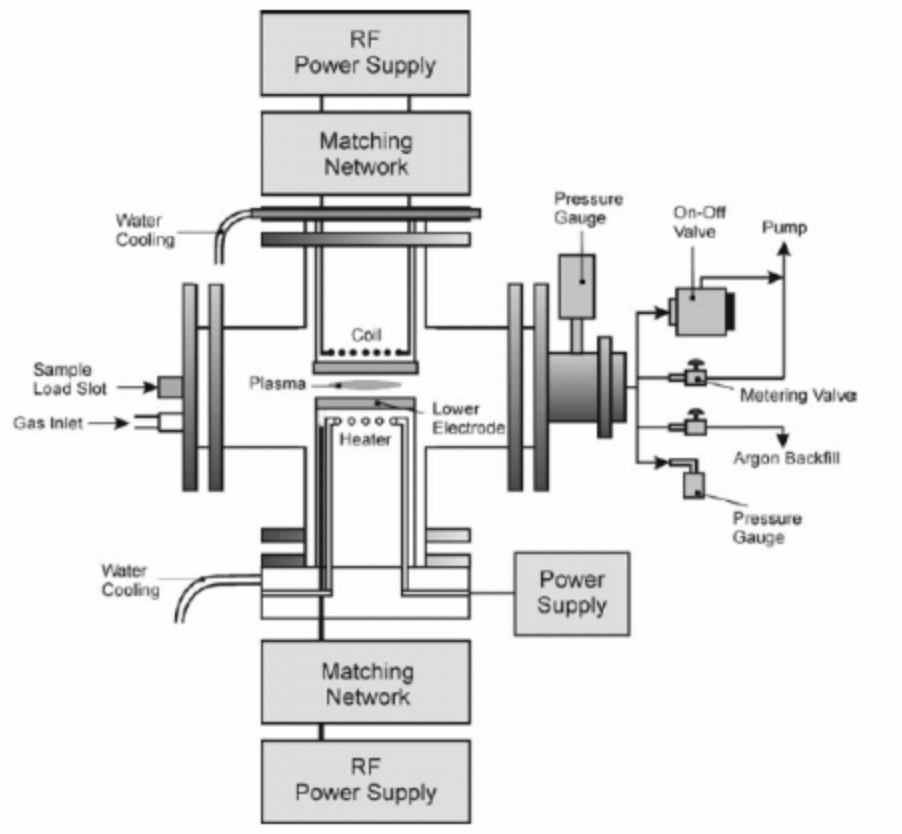


Figure 2.8 Plasma enhanced CVD schematic diagram to growth CNTs [46]

The chamber pressure can typically take a value between 1 to 20 mTorr during the experiment. The feed gas can be acetylene, methane, ethylene, ethane, or carbon monoxide, and enters the chamber from one of the parallel plate electrodes that does not hold the substrate. The energy of the plasma helps the carbon(C) molecules turn into reactive atoms, and CNTs are grown on the metal or metal alloy catalyst particles that sputtered on the substrate. Extremely dense vertical CNTs can be synthesized by PECVD method, since a local electrical field can be generated between the substrate holder and the plasma. The other advantage of the PECVD technique is the CNT growth can be achieved at the low temperatures in comparison to the other growth mechanisms. This

property gets the PECVD method one step forward for the possible integration of CNTs with semiconductor device applications.

Chapter 3

CNTs Fabrication and Characterization

3.1 Overview

Randomly aligned Carbon Nano Tubes (CNTs) are synthesized by using chemical vapor deposition technique in this thesis. Silicon (Si) and Nickel (Ni) are used as the substrate to grow CNTs. A metal catalysis is deposited onto the substrate using a radio frequency/direct current (RF/DC) sputtering system. The sputtering chamber is capable of reaching 5×10^{-6} Torr pressure and both RF and DC sputtering are feasible. However, in this work only the DC sputtering is utilized because of the choice of the metal target materials. The silicon substrate is n-type silicon with $\langle 100 \rangle$ orientation and has SiO_2 pre-coating on it. In some cases, the substrate has been treated with heat or by other means. The substrate is classified as “untreated”, when no treatment is applied. Thin films of Iron (Fe), Carbon (C) and Nickel (Ni) are deposited as catalysts or underlayers for the catalyst onto substrates. The distance between the sputtering gun and the sample was kept constant at 20 cm, and the pressure was kept at 7 mTorr during the metal deposition. Argon (Ar) gas is used as the background gas forming the plasma for deposition. Depending on the desired thickness of the metal film, the sputtering deposition time is varied. After the deposition, the substrate with the catalyst layer(s) transferred to the thermal chemical vapor deposition (CVD) chamber. The CVD chamber is capable of reaching 1100°C maximum temperature, but it was kept constant at 700°C during the CNT growth process. The chamber is a quartz tube with diameter of 2 inch, with heating

element wrapped around it is forming the furnace. Tube chamber is pumped down to a base pressure of 10^{-3} Torr using a mechanical pump initially, and then, filled with the feed gas. A mixture of argon (Ar) and acetylene (C_2H_2) feed gases are introduced to the chamber with a flow rate of 75 sccm / 20 sccm respectively. Gas flow is controlled by a mass flow controller and a pressure of 70.8 mTorr is maintained in the chamber for 20 minutes for chemical vapor deposition of CNTs.

3.2 Wafer Cleaning and Catalyst Deposition

The Si wafer is cleaned with diluted HF solution and DI water before the sputtering process to remove the impurities and native oxides. Then, it is put in an oven for dehydration bake at $120^{\circ}C$ for 20 minutes, in order to get rid of all the moisture on the wafer surface. It is then ready to load into the sputtering chamber. A 2-inch diameter Fe, Ni, and C targets are used as the catalysts to deposit onto the surface of wafer using DC sputtering. The substrate is mounted 20 centimetres over the plasma (ion) gun, which is an ion source without a filament, and works with microwave plasma discharge principle. A picture and an illustration of the sputtering chamber are shown in Figure 3.1. The chamber is then pumped down to the pressure of 5×10^{-6} Torr. Argon is fed in to the chamber, and the chamber pressure is maintained at 7 mTorr. The plasma is generated with DC/RF power that is applied to the plasma gun. The metal atoms sputtered from the target to the substrate, and a metal layer is obtained on the substrate surface at the end of the process. Sputtering times are varied between 1 to 15 minutes depending on the required catalyst thickness. An SEM image of 5 minutes Fe catalyst uniformly sputtered onto a Si substrate is shown in Figure 3.2.

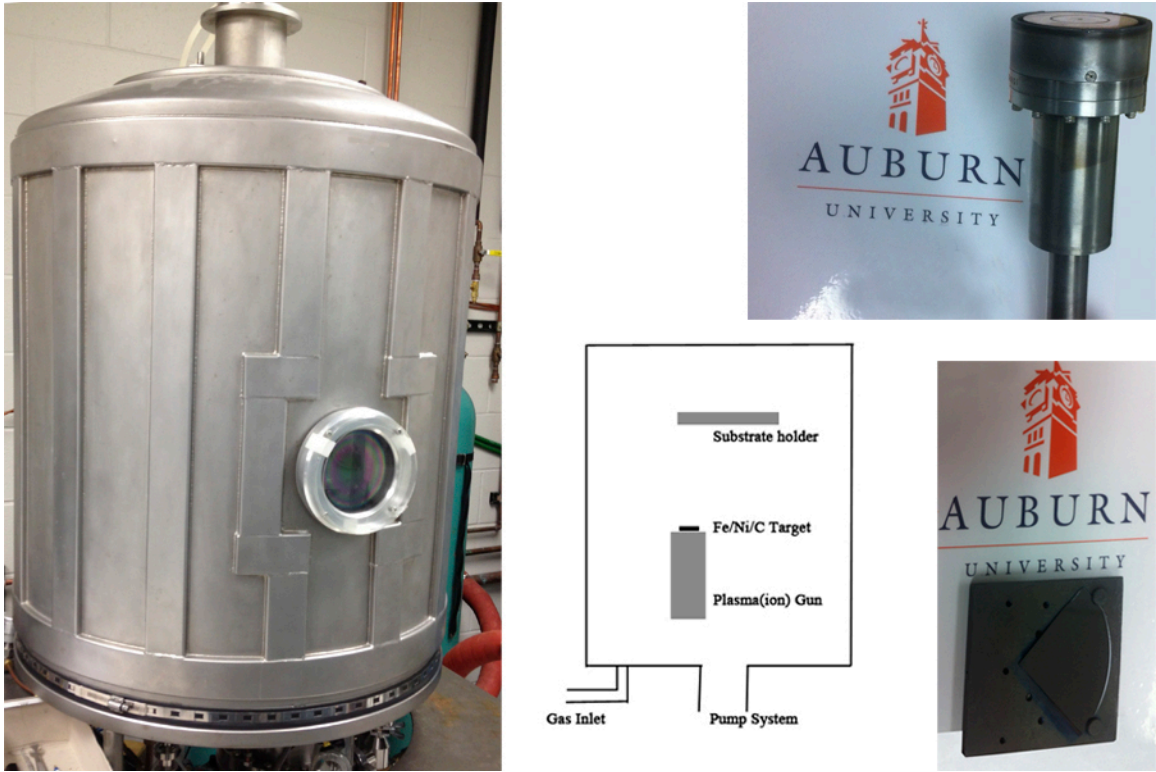


Figure 3.1 Schematic and picture of DC/RF Sputtering Chamber, Plasma gun, and substrate holder

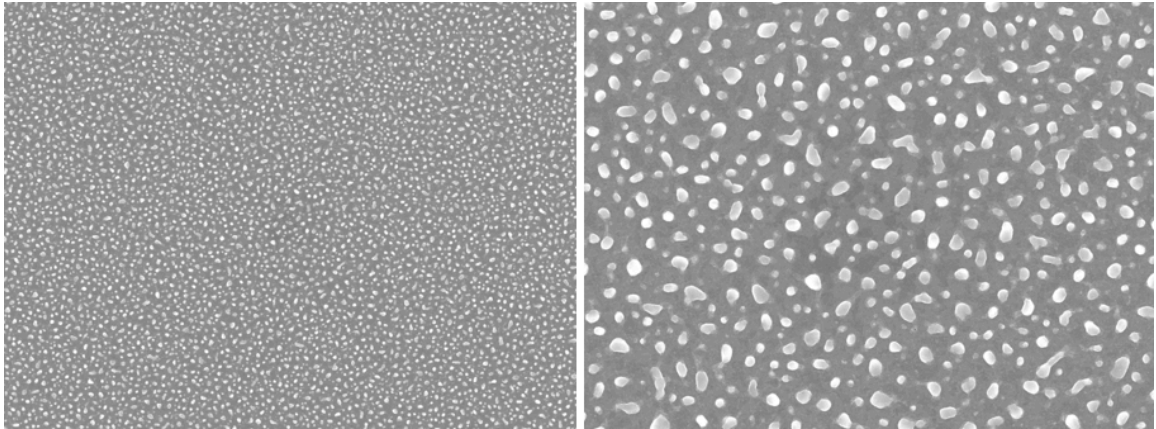


Figure 3.2 x2000 and x7000 SEM images of 5 minutes iron (Fe) sputtered Silicon substrate surface [54]

3.3 Patterning and Masking Process

Patterned CNTs are also synthesized by using chemical vapor deposition technique on Si substrate. Two different sizes of masks are used to generate the patterns. The first mask had 0.5 cm^2 by 0.5 cm^2 holes, and the second one had 0.35 cm^2 by 0.35 cm^2 holes. The Si wafers are first cleaned in Hydrogen Fluoride (HF): Water (1: 50, respectively) solution, and then are put in the oven for dehydration bake for 20 minutes at 120°C . Hexamethyldisilazane (HMDS) vapor prime is applied for 5 minutes as an adhesion promoter to the photoresist (PR). Positive – tone photoresist (AZ 5214) is then applied to the wafers for 30 seconds at 3000 rpm spin speed. After the photoresist step, the wafers are soft baked at 105°C for 1 minute. The proper mask is selected and the wafers are exposed to the UV light for 10 seconds in order to remove the PR. AZ 400K solution is used as the developer, and the wafers are developed for 18 seconds in 2: 1 (Water: AZ400K) concentration. The patterns then become visible as seen in Figure 3.3.

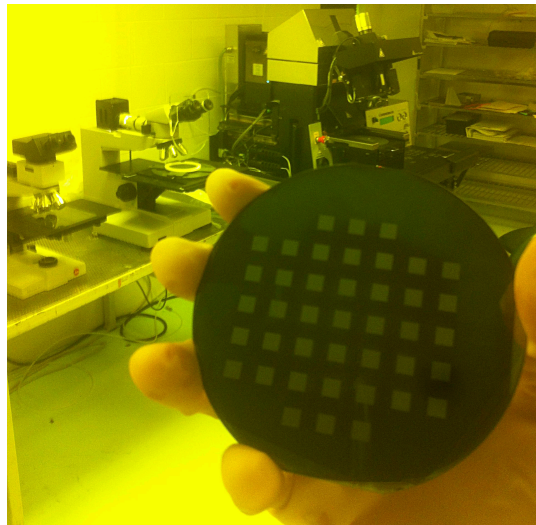


Figure 3.3 The patterned Si substrate by 0.5 cm^2 holes after the development step. (This patterned wafer is fabricated in – house)

A hard bake at 120⁰C for 1 minute follows after the development step. The wafers are exposed to the plasma for 14 seconds in order to clean the wafer surface. The wafers are then etched 20 μm by using wet and dry etching, and are put into the sputtering chamber. The similar sputtering and CVD furnace steps are followed, and CNTs are synthesized at the desired patterns as seen in Figure 3.4.

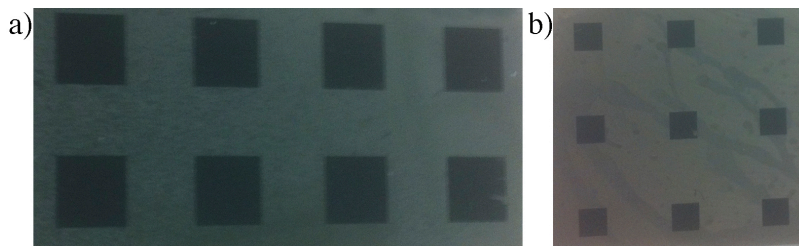


Figure 3.4 a) CNTs on Si substrate by 0.5 cm² holes after 5 minutes Fe sputtering and 20 minutes CVD growth. b) CNTs on Si substrate by 0.5 cm² holes after 5 minutes Fe sputtering and 20 minutes CVD growth. (Growth conditions were 700⁰C, 70.8 mTorr, and the Ar : C₂H₂ rate was 75sccm : 20sccm)

An illustrated flow chart of the all explained steps can be seen in Figure 3.5.

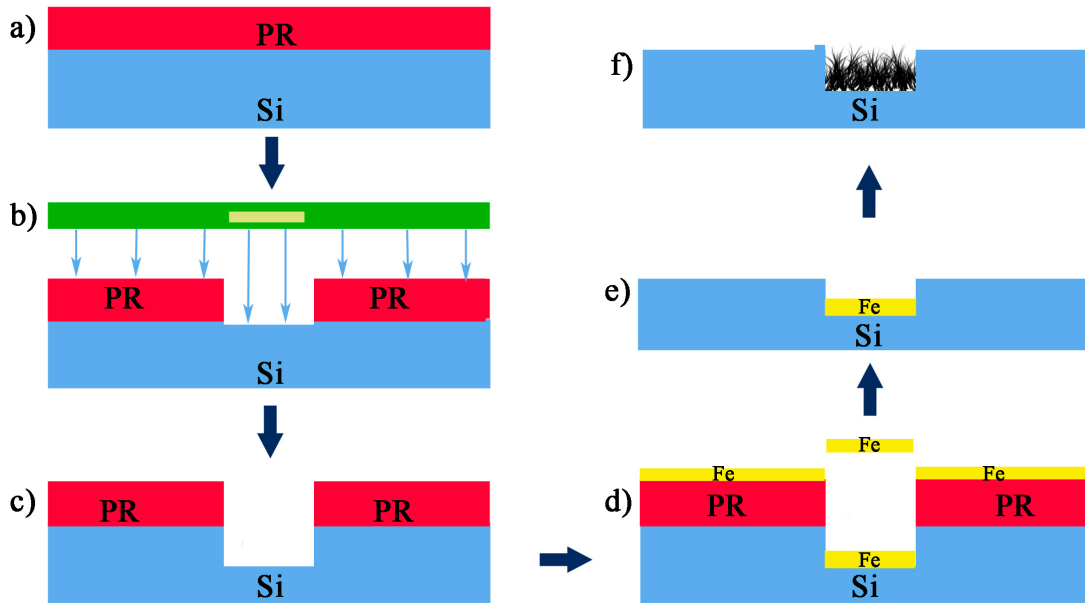


Figure 3.5 Illustrated flow chart of patterned CNT synthesis. a) Positive – tone photoresist step. b) Mask alignment step. c) Dry and wet etching. d) 5 minutes Fe sputtering. e) Removing the PR. f) CVD growth

3.4 Nickel as a Substrate to Grow CNTs

A Nickel foil is also used as a substrate. Fe is used as the catalyst to deposit onto the surface of the Ni foil using DC sputtering. Different sputtering times are used between 1 to 15 minutes in order to experience the different catalyst thickness affects. It is concluded that, although some formations of CNTs found with carbon clusters under the SEM, the results were very poor. It's decided to use SiO₂ under layer to improve the results; however, this experiment is not included in this thesis. Figure 3.6 shows Fe catalyst sputtered for 5 minutes on Ni Foil.

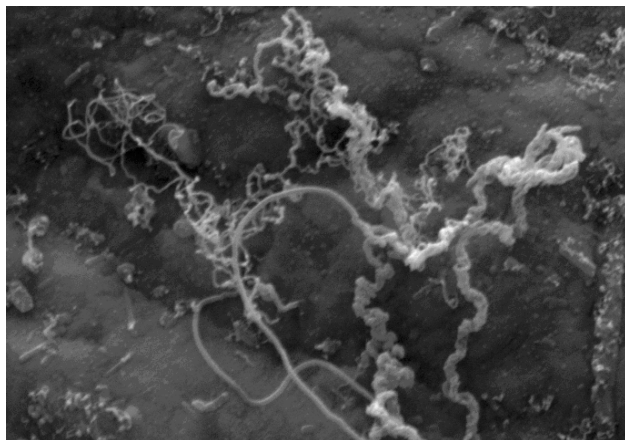


Figure 3.6 Fe catalyst sputtered for 5 minutes on Ni Foil (resolution x20k)

3.5 CNT Growth Process in CVD

After the sputtering process the silicon substrate is loaded in the thermal CVD reactor to synthesize CNTs. The quartz tube furnace is the chamber of the system. An adjustable resistive heater is used to heat the furnace to the experiment temperatures. The experiment temperatures are measured by a thermocouple that is connected to the substrate holder. Acetylene/Argon gas mixture is introduced in to the chamber with a flow rate of 20 sccm / 75 sccm respectively. The flow rates inside the thermal CVD system are measured by a flow meter that is connected to the system through the feeding gas cylinders. The pressure in the chamber is controlled by a valve that is connected to a pressure gauge and a mechanical pump. The experiment conditions of synthesis of CNTs were maintained at a growth temperature of 700°C and at the growth pressure of 70.8 Torr. An illustration of the system is shown in Figure 3.6 [47].

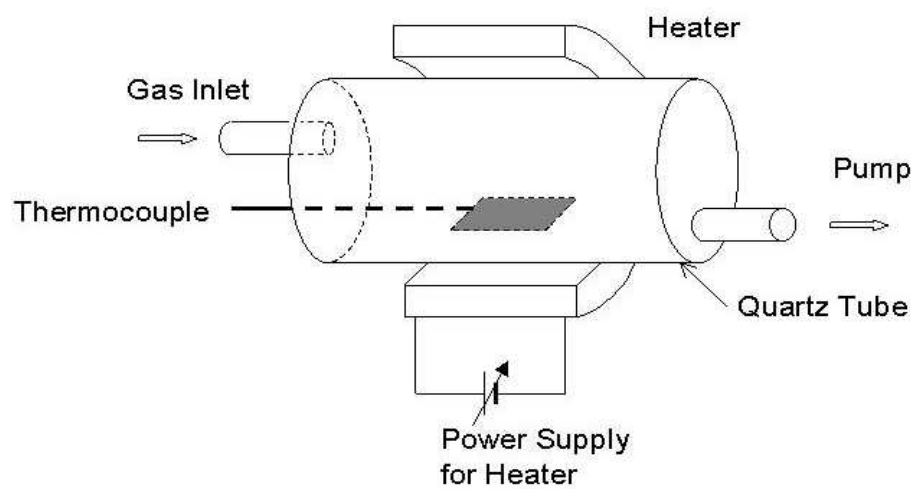


Figure 3.7 A schematic diagram of the thermal CVD system [47]

Chapter 4

Results and Discussion

4.1 - Catalyst Thickness Effect

The catalyst thickness is one of the critical parameters that affect CNT density as well as diameter and length. It was found that less than 7 nm thickness of Fe results in the growth of inhomogeneous regions of randomly aligned CNTs. On the other hand, more than 12 nm thickness of Fe results in clustered carbon/graphite growth. Two SEM pictures are seen in Figure 4.1 for Fe, and Ni catalysts with different catalyst thicknesses.

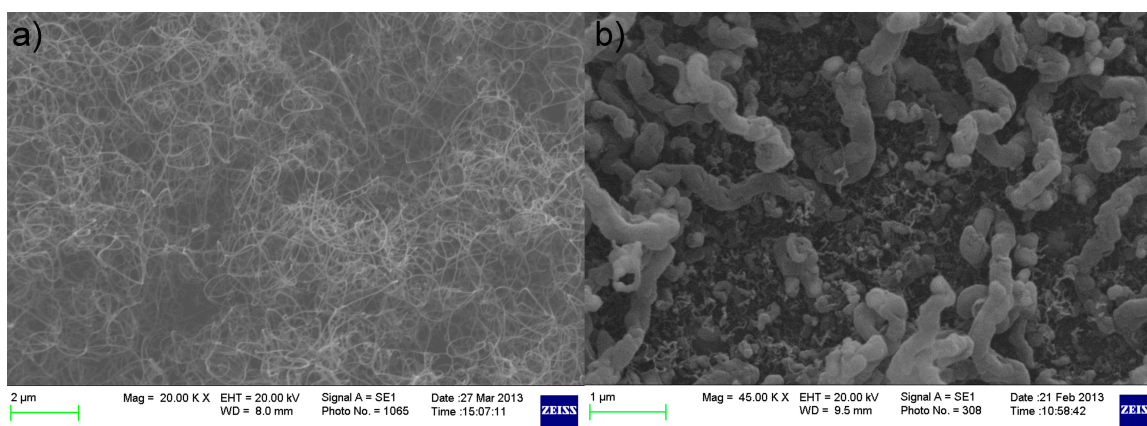


Figure 4.1 a) 10 nm deposition thickness of Fe results with very dense CNTs on Si substrate. b) <10 nm deposition thickness of Ni results with mostly carbon clusters and weak CNTs on Si substrate. (Both pictures are taken after 20 minutes CVD growth. Growth conditions were 700⁰C, 70.8 mTorr, and the Ar : C₂H₂ rate was 75sccm : 20sccm.)

It was also found from the results that a secondary level of C deposited over Fe improves the CNT growth as seen in Figure 4.2.

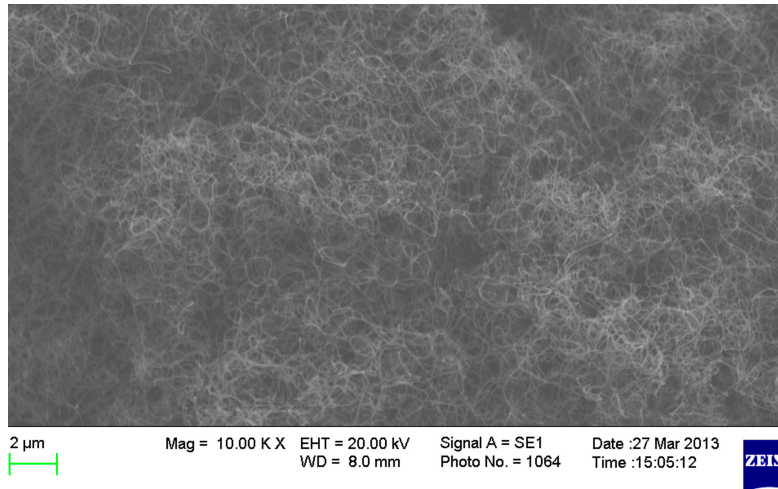


Figure 4.2 8 minutes C sputtering on already 5 minutes Fe sputtered Si substrate. (Picture is taken after 20 minutes CVD growth. Growth conditions were 700⁰C, 70.8 mTorr, and the Ar : C₂H₂ rate was 75sccm : 20sccm.)

Likewise, the Ni thickness differences were concluded with distinctive results. It was found that if the Ni thickness is more than 10 nm, there is no uniform CNT growth achieved, but mostly carbon clusters with a small amount of random growth CNT islands as shown in Figure 4.1b. Although CNTs were grown less than stated thickness, the results were poor. That might be due to the Nickel Silicide (NiSi) formation favorable for temperatures of over 300⁰C as explained by Ducati et al [48]. So, in order to prevent this formation SiO₂ underlayer is used between the Ni catalysis and the substrate.

Although the results were improved as shown in Figure 4.3a, the results were not at the desired level. Therefore, an 8 hours annealing process at 300⁰C was applied to substrate with the SiO₂ coating as a pretreatment. Then a layer of Fe was sputtered on top of the Ni deposited substrate that has the SiO₂ as the under-layer. Those treatments

improved the density of CNTs and helped the growth with the same synthesizing conditions explained above. One example is shown in Figure 4.3b. The effect of the annealing process between the Ni and Fe sputtering also was studied, however, this treatment did not improve the results as it is seen in Figure 4.3c.

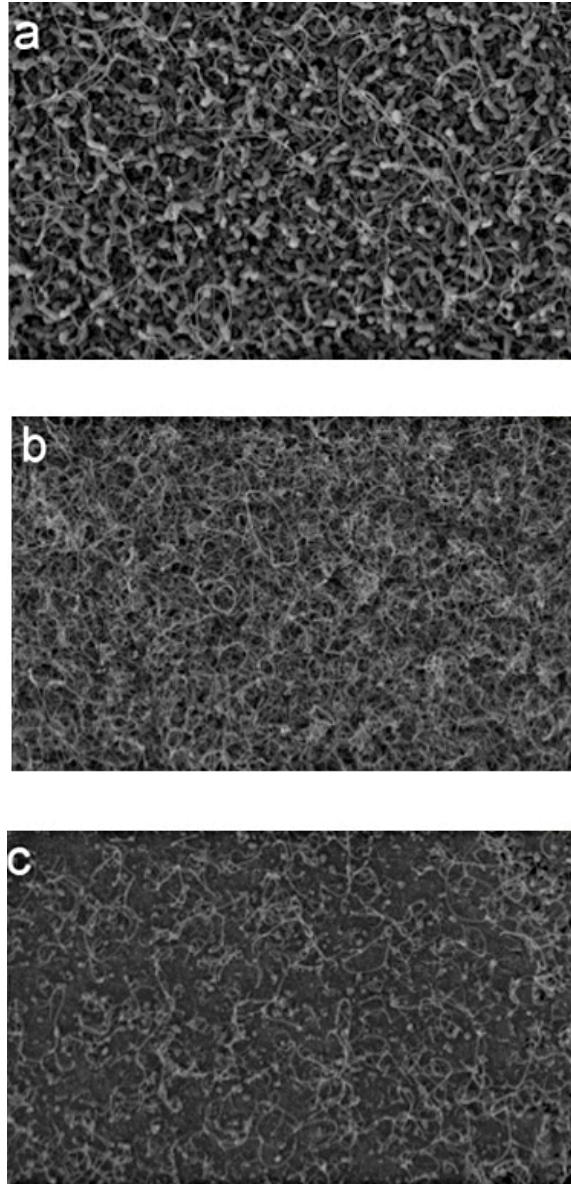


Figure 4.3: a) Ni 5 minutes, and Fe 5 minutes sputtering on SiO₂ b) Pretreated Ni 5 minutes, and Fe 5 minutes sputtering on SiO₂ c) Ni 7 minutes sputtering, 8 hours annealing, and Fe 5 minutes sputtering respectively on SiO₂ (All pictures are taken after 20 minutes CVD growth. Growth conditions were 700⁰C, 70.8 mTorr, and the Ar : C₂H₂ rate was 75sccm : 20sccm.)

It is concluded that although the pretreatment improved the density of CNTs, the formation was inhomogeneous on some regions of the substrate as shown in Fig 4.4.

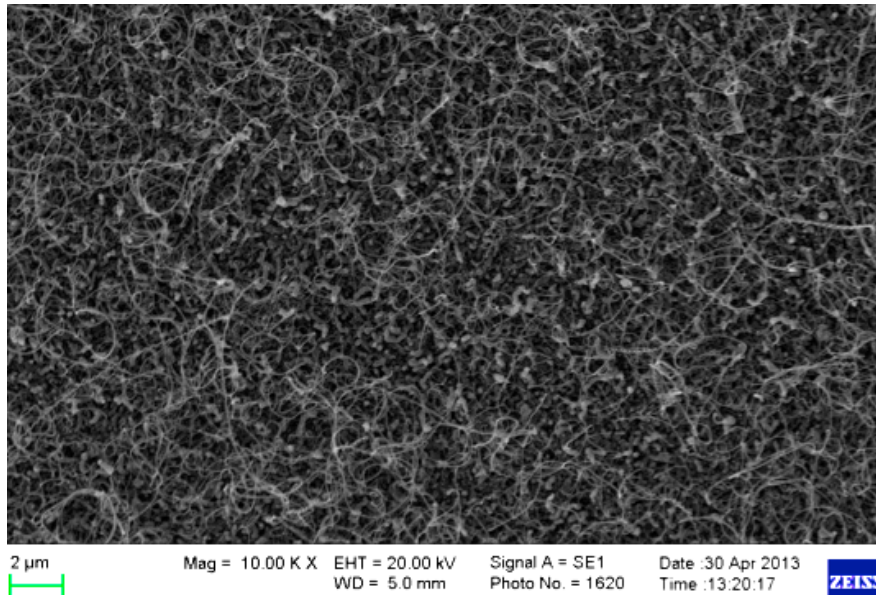


Figure 4.4: Left side of the substrate respect to the Fig 3b -Ni 5 minutes, and Fe 5 minutes sputtered SiO₂ sample. - (Picture is taken after 20 minutes CVD growth. Growth conditions were 700⁰C, 70.8 mTorr, and the Ar : C₂H₂ rate was 75sccm : 20sccm.)

4.2 - DC/RF Sputtering Distance and Pressure Effect

Sputtering distance was kept constant at 20 cm in this paper, and sputtering pressure controlled from 3 mTorr to 15 mTorr ranges. Sputtered catalyst thicknesses for Fe were measured and given at Table 1 for t = 5 minutes. It is studied that higher than 7 mTorr pressures are caused larger thicknesses. This larger catalyst thickness resulted with graphite growth instead of CNTs. In contrast, if the catalyst is deposited at the pressures of lower than 7 mTorr, then the formation of CNTs were seen, however, the tubes were weak (thin), and inhomogeneously formed on the surface. The measured catalyst

thicknesses corresponding these deposition conditions were lower at these relatively low pressures.

Sputtering Time / Pressure	10 mTorr	7 mTorr	5 mTorr	3mTorr
t = 5 mins	45 nm	12 nm	7nm	5nm

Table 4.1 Varying layer thicknesses depending on the sputtering pressure.

4.3 - Flow Rate Effect

A flowing mixture of acetylene (C_2H_2) and argon (Ar) is used to grow CNTs. It is decided that best results achieved by the flow rate of C_2H_2 , 20 sccm; and Ar, 75 sccm. The chamber pressure is fixed to 70.8 mTorr during the growth process, and temperature of $700^{\circ}C$ is used for Fe, Ni, and secondary layered (Fe - C and Ni - Fe) catalyst – coated Si substrates. Although some carbon clusters are presented, the tube density was the highest. The growth time was 20 minutes, and it is only affected the carbon nanotubes' lengths.

4.4 - CVD Temperature Effect

Most of the CNT synthesis is carried out at the deposition temperature of $700^{\circ}C$. Deposition temperatures of lower than $700^{\circ}C$ are resulted with very low density CNT growth. It is speculated that the decomposition of acetylene (C_2H_2) is not efficient at these low temperatures. Furthermore, at higher temperatures than $700^{\circ}C$, CNT deposition

process is resulted with weak CNT growth too. So, it can be assumed that the growth rate of CNTs is as a function of temperature initially increases, and then decreases as the temperature increases beyond 700° in our system.

4.5 – SEM Images (collection)

In this section, the scanning electron microscope (SEM) images of CNT samples with different growth conditions and underlayers are presented. The Figure 4.5, 4.6, and 4.7 SEM images show that the samples with 5 minutes Fe sputtering time on Si substrate, and with 1 and 5 minutes Fe sputtering time on SiO₂. Figure 4.8, 4.9, and 4.10 show that Ni sputtering on Si substrate results with carbon clusters. That might be due to the Nickel Silicide (NiSi) formation favorable for temperatures of over 300⁰C as it is stated earlier at this section, and explained by Ducati et al [48]. Figure 4.11 shows that Ni sputtering on top of the 5 minutes Fe sputtering can be resulted with some weak formations of CNTs. The sample with 5 minutes Fe and 8 minutes C sputtering time can yield very good-quality, and almost vertically aligned MWCNTs as shown in Figure 4.12. Figure 4.13 shows an experiment to growth CNT on Ni Foil. A successful CNT growth on SiO₂ substrate with 5 minutes Ni and 5 minutes Fe sputtering can be seen in Figure 4.14. When the Ni sputtering time is increased to 7 minutes and then 10 minutes as it seen in Figure 4.15 and 4.16 respectively, the catalyst thickness goes too thick. Therefore, some carbon clusters will be formed instead of CNTs. Lastly, the cross-sectional, and side SEM images of randomly oriented MWCNTs of patterned Si substrates are presented in Figure 4.17 and 4.18.

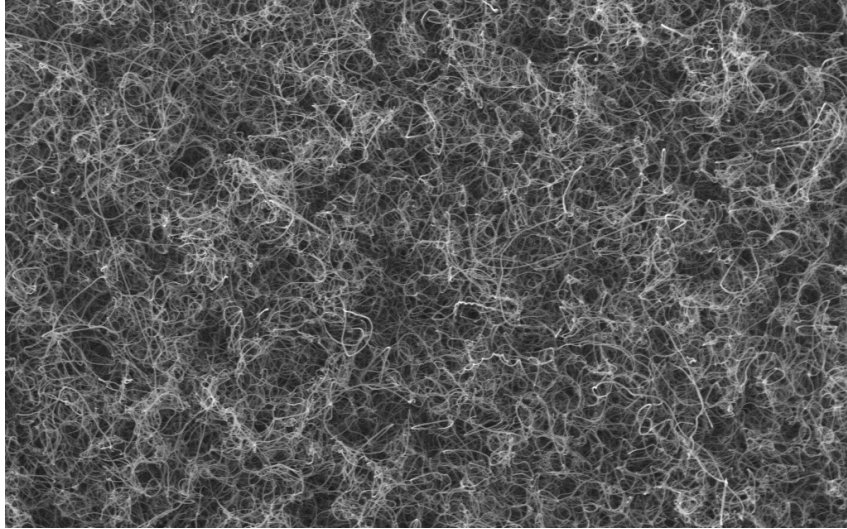


Figure 4.5 Randomly oriented CNTs grown of Fe catalyst sputtered for 5 minutes on Si substrate (resolution x10k)

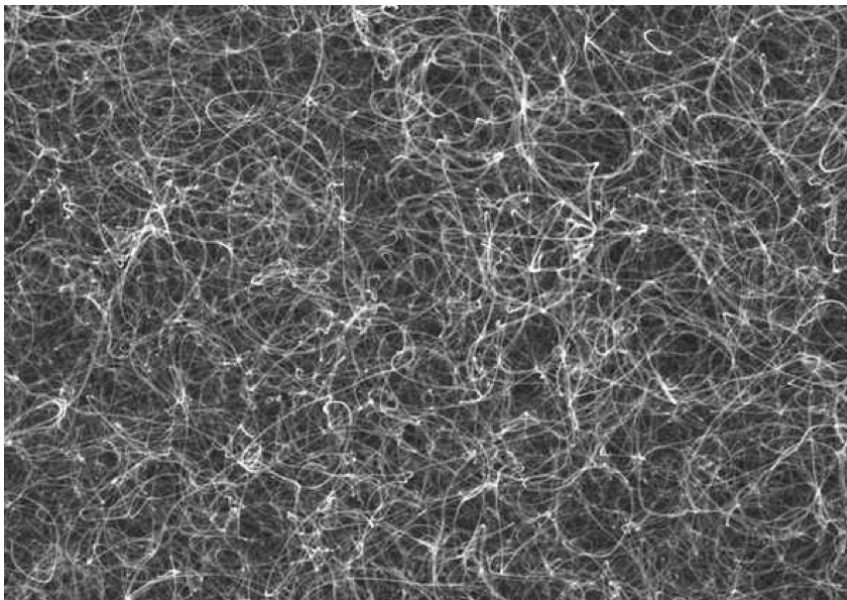


Figure 4.6 Randomly oriented CNTs grown of Fe catalyst sputtered for 1 minute on SiO₂ substrate (resolution x10k)

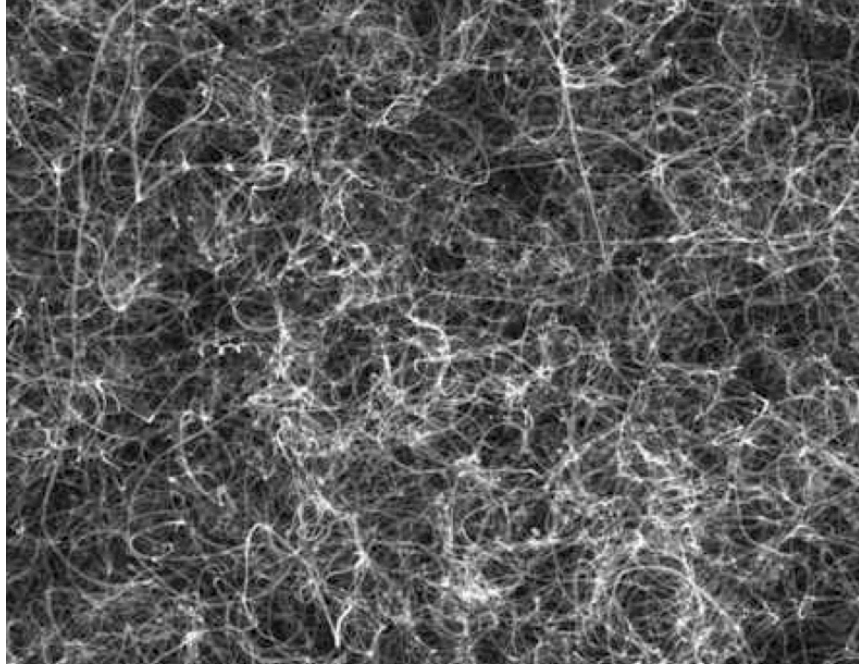


Figure 4.7 Randomly oriented CNTs grown of Fe catalyst sputtered for 5 minutes on SiO_2 substrate (resolution x10k)

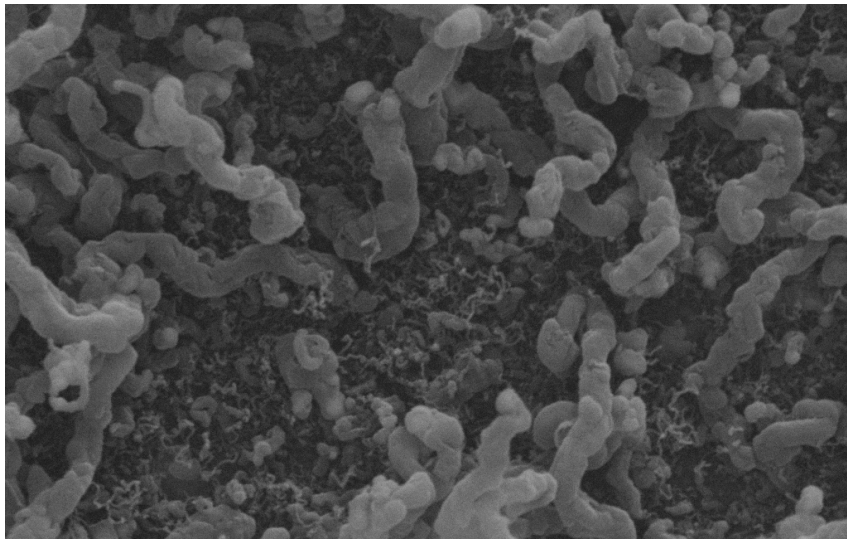


Figure 4.8 Ni catalyst sputtered for 5 minutes on Si substrate (resolution x50k)



Figure 4.9 Ni catalyst sputtered for 5 minutes on top of the Fe catalyst sputtered for 5 minutes Si substrate (resolution x30k)

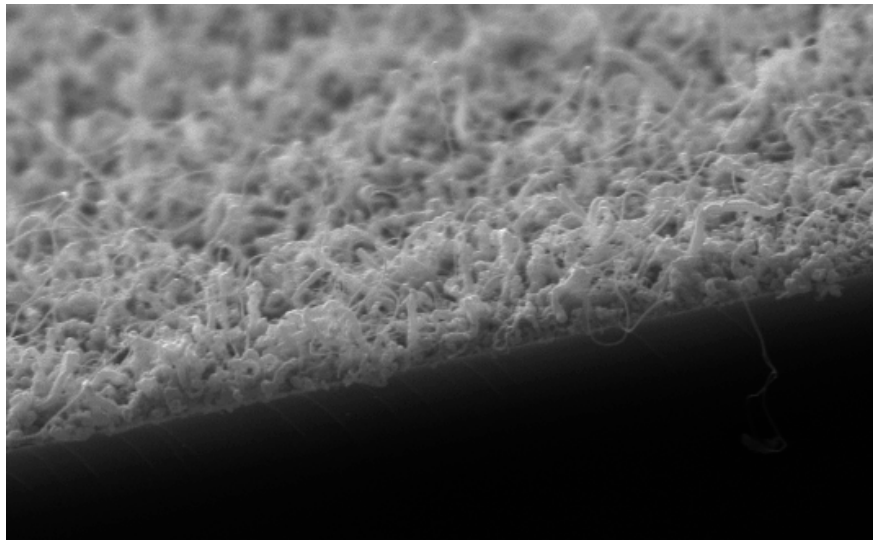


Figure 4.10 Cross – sectional image of Ni catalyst sputtered for 3 minutes on top of the Fe catalyst sputtered for 5 minutes Si substrate (resolution x20k)

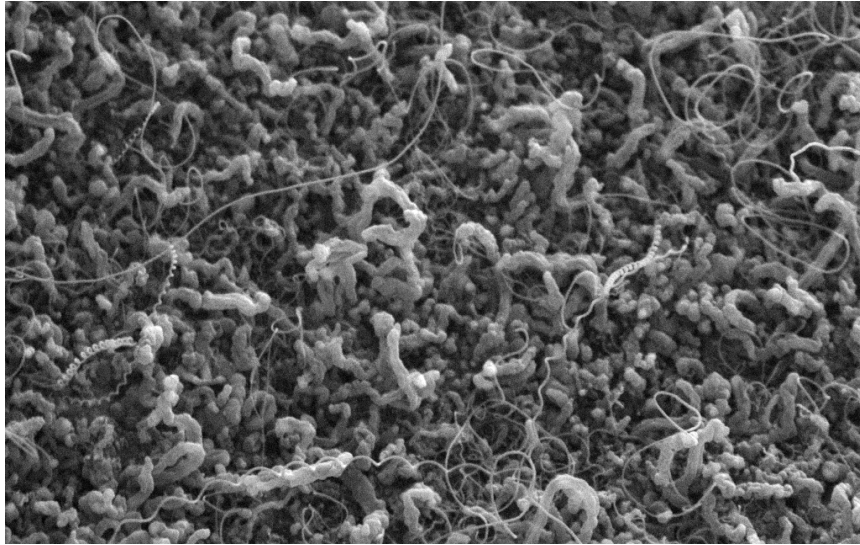


Figure 4.11 Ni catalyst for 3 minutes, Fe catalyst for 5 minutes, and C catalyst for 8 minutes sputtered on Si substrate (resolution x30k)

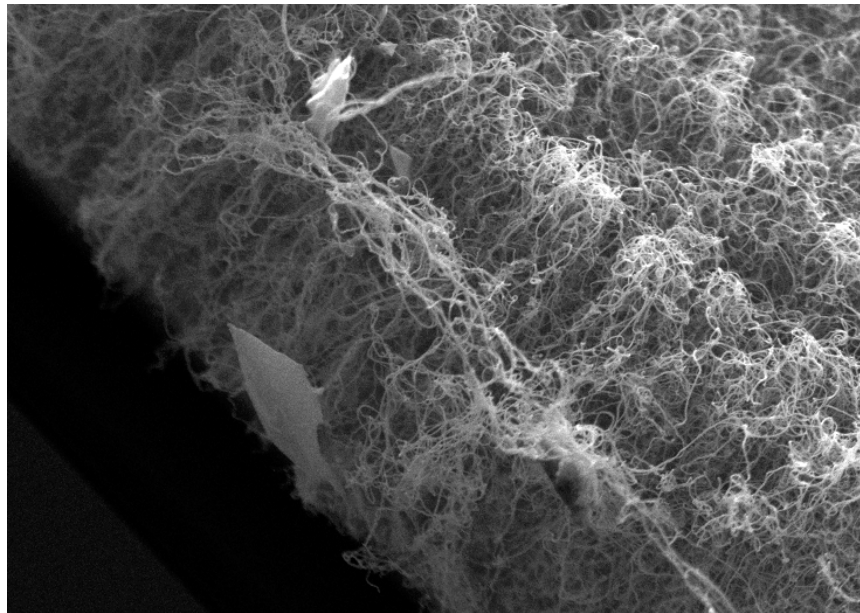


Figure 4.12 Cross – sectional image of C catalyst sputtered for 8 minutes on top of the Fe catalyst sputtered for 5 minutes Si substrate (resolution x10k)

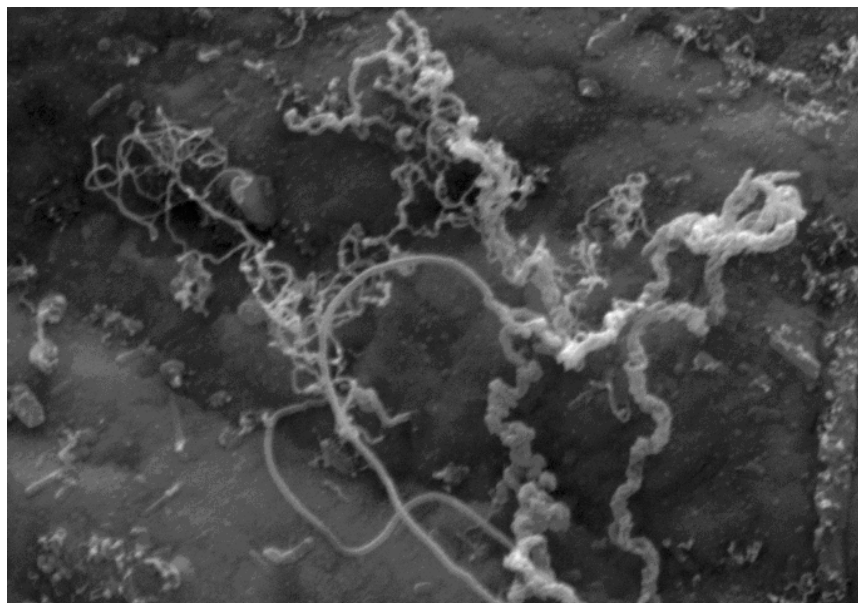


Figure 4.13 Fe catalyst sputtered for 5 minutes on Ni Foil (resolution x20k)

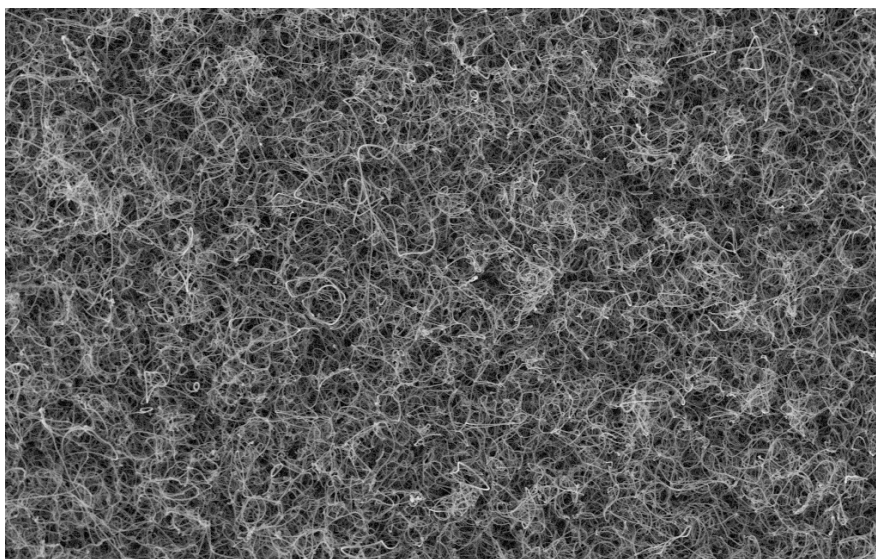


Figure 4.14 Ni catalyst sputtered for 5 minutes on top of the Fe catalyst sputtered for 5 minutes SiO₂ substrate (resolution x10k)

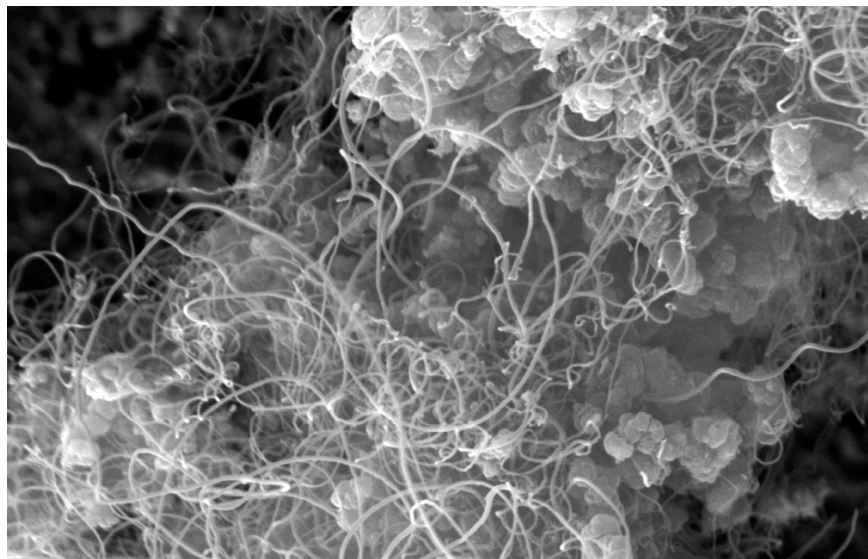


Figure 4.15 Ni catalyst sputtered for 7 minutes on top of the Fe catalyst sputtered for 5 minutes SiO₂ substrate (resolution x20k)

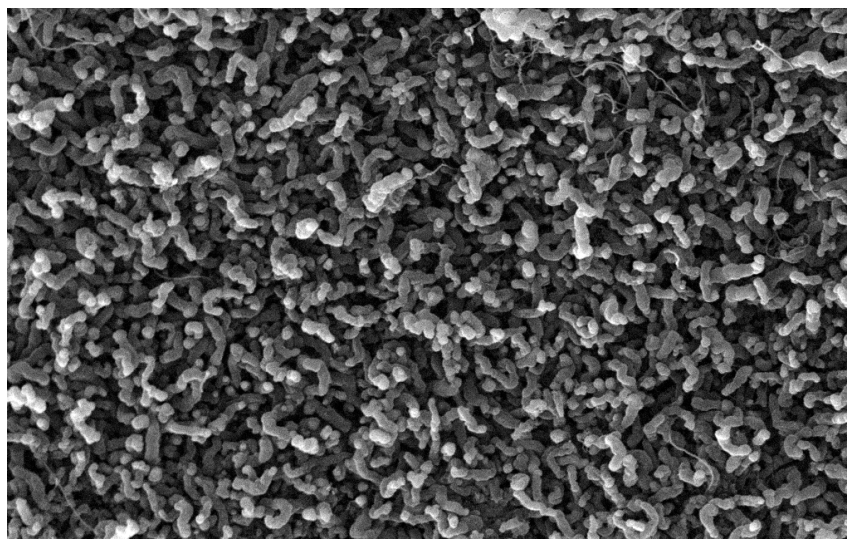


Figure 4.16 Ni catalyst sputtered for 10 minutes on top of the Fe catalyst sputtered for 5 minutes SiO₂ substrate (resolution x20k)

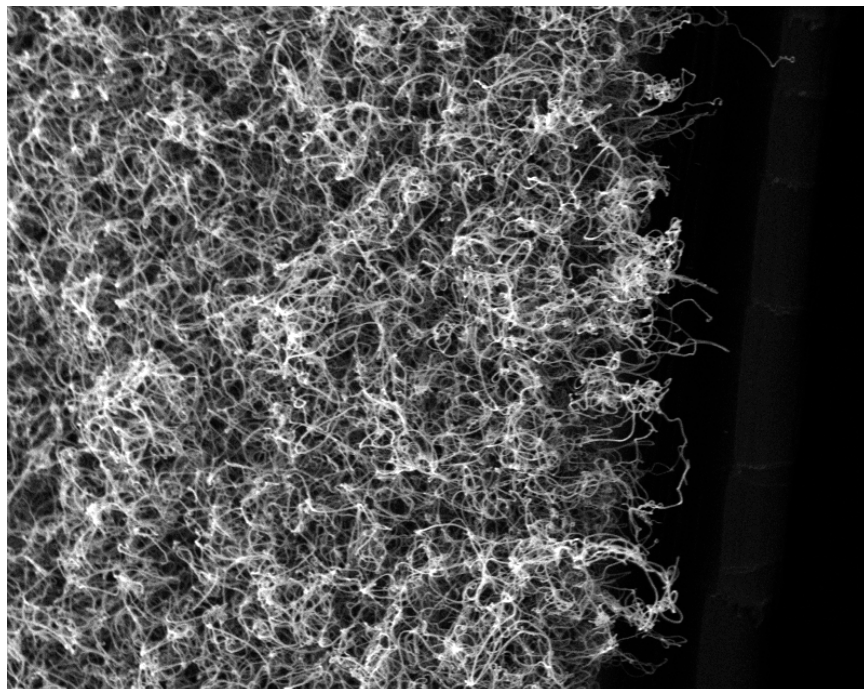


Figure 4.17 Side image of Fe catalyst sputtered for 5 minutes on $.5 \text{ cm}^2 \times .5 \text{ cm}^2$ patterned Si substrate (resolution x10k)

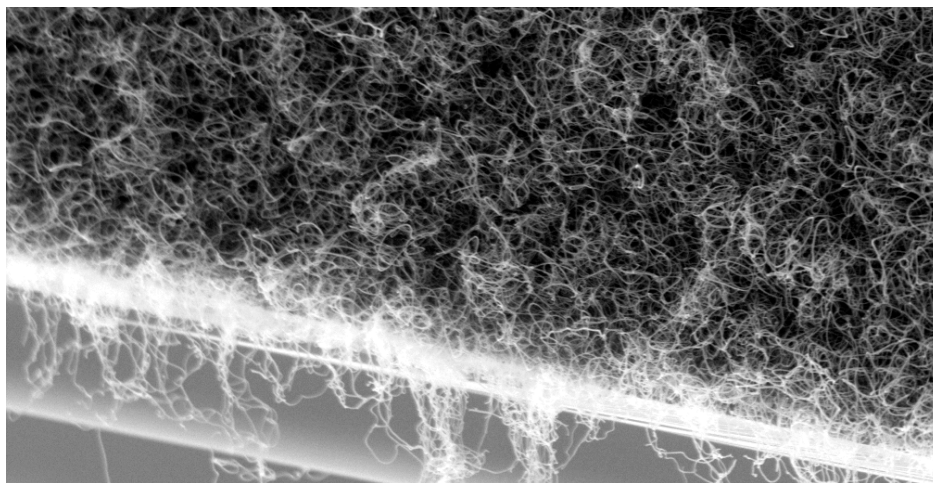


Figure 4.18 Cross – sectional image of Fe catalyst sputtered for 5 minutes on $.35 \text{ cm}^2 \times .35 \text{ cm}^2$ patterned Si substrate (resolution x10k)

Chapter 5

Conclusions

In this thesis, selective and non – selective randomly oriented multi – wall carbon nanotubes are synthesized. Their electrical and thermal properties are also investigated. Different metals namely Fe, Ni and C are sputtered as catalysts on Si, Ni, and SiO₂ coated Si substrates. From the experimental results, it is concluded that the catalyst thickness, sputtering distance and background pressure during the sputtering are key parameters to grow CNTs. The CNTs are grown by chemical vapor deposition (CVD) method. The CVD furnace temperature and gas flow rates also played important roles in the synthesise process. Moreover, results show that the electrical and thermal properties of CNTs change depending on the growth process and conditions.

The patterned CNTs are also studied and the fabrication process is clearly explained in this work. Advantages of CVD technique are seen in the experiment results. Controllable growth and mass production capabilities give a priority to this technique. It can be safely said that this technique is the most probable method to synthesise CNTs for many future applications.

REFERENCES

- [1] Iijima, S., “*Helical microtubules of graphitic carbon*” *Nature* 354, pp.56 – 58 1991
- [2] Yograj Singh Duksh, Brajesh Kumar Kaushik, Sankar Sarkar, Raghuvir Singh, “*Performance comparison of carbon nanotube, nickel silicide nanowire and copper VLSI interconnects: Perspectives and challenges ahead*”, *Journal of Engineering, Design and Technology*, Vol. 8 Iss: 3, pp.334 – 53, 2010
- [3] Thomas, Jim, et al. “*Nanotechnology*.” *The Ecologist*. May, 2003.
- [4] S. J. Tans, A. R. M. Verschueren, and C. Dekker, “*Room – temperature transistor based on a single carbon nanotube*”, *Nature (London)*, vol.393, 49, 1998
- [5] A. Javey, J. Guo, Q. Wang, M. Lundstrom, H. J. Dai, “*Ballistic carbon nanotube field – effect transistor*”, *Nature*, vol.424, pp.654 – 57, 2003
- [6] C. Lu, Q. Fu, S. Huang, and J. Liu, “*Polymer Electrolyte – Gated carbon nanotube field – effect transistor*”, *Nano Lett*, vol.4, pp. 623 – 27, 2004
- [7] S. J. Tan, M. H. Devoret, H. J. Dai, A. Thess, R. E. Smalley, L. J. Geerligs, and C. Dekker, “*Individual single wall carbon nanotubes as quantum wires*”, *Nature (London)*, vol.386, pp.474 – 77, 1997
- [8] M. Bockrath, D. H. Cobden, and P. L. McEuen, *Science* 290, 1552, 2000
- [9] J. Kong, N. R. Franklin, C. Zhou, M. G. Chapline, S. Peng, K. Cho, and H. Dai, “*Nanotube molecular wires as chemical sensors*”, *Science*, vol.287, pp.622 – 25, 2000
- [10] H. J. Dai, J. H. Hafner, A. G. Rinzler, D. T. Colbert, and R.E. Smalley, “*Nanotubes as Nanoprobes in scanning probe microscopy*”, *Nature (London)*, vol.384, pp.147 – 150, 1996
- [11] W. A. deHeer, A. Chatelain, and D. Ugarte, “*A carbon nanotube field – emission electron source*”, *Science*, vol.270, pp.1179 – 80, 1995
- [12] W. Zhu, C. Bower, G.P. Kochanski, and S. Jin, “*Electron field emission from nanostructured diamond and carbon nanotubes*”, *Solid – State Electronics*, vol.45, pp.921 – 28, 2001
- [13] B.Q. Wei, R. Vajtai, P.M. Ajayan, “*Reliability and current carrying capacity of carbon nanotubes*”, *Appl Phys Lett*, vol.79, no.8, pp.1172 – 74, 2001

- [14] Z.K. Tang, L.Y. Zhang, N. Wang, X.X. Zhang, G.H. Wen, G.D. Li et al. “*Superconductivity in 4 Angstrom single-walled carbon nanotubes*”, *Science*, vol.292 no.5526, pp.2462 – 65, 2001
- [15] P. Kim, L. Shi, A. Majumdar, P.L. McEuen, “*Thermal transport measurements of individual multi – walled nanotubes*”, *Phys Rev Lett*, vol.87, pp.215502–216606, 2001
- [16] Zhu, Y.J., Lin, T.J., Liu, Q.X., Chen, Y.L., Zhang, G.F., Xiong, H.F., Zhang, H.Y., “*The effect of nickel content of composite catalysts synthesized by hydrothermal method on the preparation of carbon nanotubes*”, *Mater. Sci. Eng. B- Solid State Mater. Adv. Technol.*, vol.127 no.2-3, pp.198-202, 2006
- [17] J.P. Salvetat, A.J. Kulik, J.M. Bonard, G.A.D. Briggs, T. Stockli, K. Metenier et al., “*Elastic modulus of ordered and disordered multi – walled carbon nanotubes*”, *Adv. Mater*, vol.11, no.2, pp.161 – 65, 1999
- [18] Jonathan N. Coleman, Umar Khan, Werner J. Blau, Yurii K. Gun’ko, “*Small but strong: A review of the mechanical properties of carbon nanotube–polymer composites*”, *Carbon*, vol.44, Iss.9, pp.1624 – 52, 2006
- [19] J. Prasek, J. Drbohlavova, J. Chomoucka, J. Hubalek, O. Jasek, V. Adam, R. Kizek, “*Methods for carbon nanotubes synthesis-review*”, *Journal of Materials Chemistry*, vol.21, no.40, pp.15872 – 84, 2011
- [20] Bhupesh Chandra. PhD thesis, Columbia University, 2009
- [21] M. S. Dresselhaus, G. Dresselhaus, and Ph. Avouris. “*Carbon nanotubes, Topics in Applied Physics*” 2001
- [22] M.S. Dresselhaus, G. Dressehaus, R. Saito, and A. Jorio. “*Raman spectroscopy of Carbon Nanotubes*”, *Physics Reports*, 2004
- [23] T. W. Ebbesen, H. Lezec, H. Hiura, J. W. Bennett, H. F. Ghaemi, and T. Thio, “*Electrical conductivity of individual carbon nanotubes*”, *Nature*, 382, 54, 1996
- [24] Mayumi Kosaka, Thomas W. Ebbesen, Hidefumi Hiura, and Katsumi Tanigaki. “*Electron spin resonance of carbon nanotubes*”, *Chemical Physics Letters*, 1994
- [25] L. P. Biro, TS. Lazarescu, Ph. Lambin, P. A. Thiry, A. Fonseca, J. B. Nagy, and A. A. Lucas. “*Scanning tunneling microscope investigation of carbon nanotubes produced by catalytic decomposition of acetylene*”, *Physical Review B*, 1997
- [26] Ryuichi Kuzuo, Masami Terauchi, and Michiyoshi Tanaka, “*Electron Energy-Loss Spectra of Carbon Nanotubes*”, *Japanese Journal of Applied Physics*, 1992
- [27] H. S. Nalwa, editor, “*Handbook of nanostructured materials and nanotechnology*”, *Academic Press*, Vol. 5, 2000

- [28] B.Q. Wei, R. Vajtai, P.M. Ajayan “*Reliability and current carrying capacity of carbon nanotubes*”, *Applied Physics Letters*, vol.79 no.8, pp.1172–1174, 2001
- [29] J. Hone, M.C. Llaguno, M.J. Biercuk, A.T. Johnson, B. Batlogg, Z. Benes et al. “*Thermal properties of carbon nanotubes and nanotube-based materials*”, *Applied Physics A – Materials Science & Processing*, vol.74, no.3, pp. 339–343, 2002
- [30] M. Yu, O. Lourie, M.J. Dyer, T.F. Kelly, R.S. Ruoff “*Strength and breaking mechanism of multiwalled carbon nanotubes under tensile load*”, *Science*, vol.287, pp. 637–640, 2000
- [31] J.P. Salvetat, G.A.D. Briggs, J.M. Bonard, R.R. Bacsa, A.J. Kulik, T. Stockli et al. “*Elastic and shear moduli of single-walled carbon nanotube ropes*”, *Physical Review Letters*, vol.82, no.5, pp. 944–947, 1999
- [32] A. Thess, R. Lee, P. Nikolaev, H. Dai, P. Petit, J. Robert, C. Xu, Y.H. Lee, S.G. Kim, A.G. Rinzler, D.T. Colbert, G.E. Scuseria, D. Tomanek, J.E. Fischer, and R.E. Smalley, “*Crystalline Ropes of Metallic Carbon Nanotubes*”, *Science*, 273, 483, 1996
- [33] A. J. Cheng, “*Cold Cathodes for Applications in Poor Vacuum and Low Pressure Gas Environments: Carbon Nanotubes vs. Zinc Oxide Nano needles*”, Master Thesis, Auburn University, 2006
- [34] H. Hiura, T. W. Ebbesen, K. Tanigaki, “*Opening and purification of carbon nanotubes in high yields*”, *Adv. Mater.* 7, 275 (1995)
- [35] H. TA, and J. Hill, “*Modeling the Loading and Unloading of Drugs into Nanotubes*”, *Small*, Vol. 5, pp. 300-08, 2009
- [36] N. W. S. Kam, M. O’Connell, J. A. Wisdom, H. Dai, “*Carbon Nanotubes as multifunctional biological transporters and near-infrared agents for selective cancer cell destruction*”, *PNAS*, Vol. 102, pp. 11600, 2005
- [37] H. Muguruma, Y. Matsui, Y. Shibayama, “*Carbon Nanotube-Plasma Polymer-Based Amperometric Biosensors: Enzyme-Friendly Platform for Ultrasensitive Glucose Detection*”, *Japanese Journal of Applied Physics*, Vol. 46, Issue 9A, pp. 6078, 2007
- [38] J. Clendenin, J. Kim, S. Tung, “*An aligned Carbon Nanotube Biosensor for DNA Detection*”, *Proc of 2007 2nd IEEE Conference on Nanotechnology*, pp. 1028, 2007
- [39] M Terrones, “*Science and technology of the twenty-first century: Synthesis, Properties and Applications of Carbon Nanotubes*”, *Annu. Rev. Mater.Res.* , Vol. 33, pp. 419–501, 2003

- [40] T. Guo, P. Nikolaev, A. Thess, D. T. Colbert and R. E. Smalley, “*Fullerene Nanotubes in Electric-Fields*”, *Chem. Phys. Letters*, Vol. 243, pp. 49–54, 1995
- [41] M. Daenen, R.D. de Fouw, B. Hamers, P.G.A. Janssen, K. Schouteden, M.A.J. Veld, “*The Wondrous World of Carbon Nanotubes*”, *project*, 2003
- [42] M.L. Terranova¹, V. Sessal, and M. Rossi, "The World of Carbon Nanotubes: an overview of CVD Growth Methodologies", *Chemical Vapor Deposition*, Vol. 12, pp. 315–325, 2006
- [43] M. Su, B. Zheng, and J. Liu, “*A Scalable CVD Method for the Synthesis of Single Walled Carbon Nanotubes with High Catalyst Productivity*”, *Chem. Phys. Letters*, Vol. 322, pp.321-26, 2000
- [44] H. Lee, Y.S. Kang, P.S. Lee, and J. Y. Lee, “*Hydrogen Storage in Ni Nanoparticle-Dispersed Multi-walled Carbon Nanotubes*”, *J. Alloys Compd.*, Vol. 330, pp. 569-572, 2005
- [45] Ph. Mauron, Ch. Emmenegger, A. Züttel, Ch. Nützenadel, P. Sudan, L. Schlapbach, “*Synthesis of Oriented Nanotube Films by Chemical Vapor Deposition*”, *Carbon* 40, pp. 1339-1344, 2002
- [46] M. Meyyappan, editor, “*Carbon nanotubes science and applications*”, *CRC Press*, 2004
- [47] Y. Tzeng, C. Liu, C. Cutshaw, Z. Chen, “*Low temperature CVD Carbon Coatings on Glass Plates for Flat Panel Display Applications*” *Mat Res. Soc. Proc*, Vol 621, 2000
- [48] M. Chhowalla, K. B. K. Teo, C. Ducati, N. L. Rupesinghe, G. A. J. Amaratunga, A. C. Ferrari, D. Roy, J. Robertson, and W. I. Milne, “*Growth process conditions of vertically aligned carbon nanotubes using plasma enhanced chemical vapor deposition*” *Journal of Applied Physics*, Vol. 90, No. 10, pp5308-17, 2001
- [49] Bower Chris, Zhu Wei, Jin Sungho, Zhou Otto, “*Plasma-induced alignment of carbon nanotubes*” *Journal of Applied Physics* Vol. 77, No. 6, pp830-32, 2000
- [50] Chunsheng Du, Ning Pan, “*CVD growth of carbon nanotubes directly on nickel substrate*” *Materials Letters*, Vol.59, pp1678-82, 2005
- [51] Chung – Nan Tsai, “*Selective and Non-selective Synthesis of Carbon Nanotubes (CNTs) by Chemical Vapor Deposition (CVD) Characterization: Catalysts and Underlayers Effects on Field Emission Properties*”, *Master Thesis, Auburn University*, 2012
- [52] V. I. Merkulov, D. H. Lowndes, Y. Y. Wei, G. Eres, and E. Voelkl, “*Patterned growth of individual and multiple vertically aligned carbon nanofibers*” *Journal of Applied Physics*, Vol. 76, No. 24, pp3555-58, 2000

- [53] Hou T. Ng, Bin Chen, Jessica E. Koehne, Alan M. Cassell, Jun Li, Jie Han, and M. Meyyappan, “*Growth of Carbon Nanotubes: A Combinatorial Method To Study the Effects of Catalysts and Underlayers*” *Journal of Physical Chemistry*, Vol. 107, No. 33, pp8484-89, 2003
- [54] Haitao Zhao, “*Design and Construction of CNTs Triggered Pseudospark Switch*” *PhD Dissertation, Auburn University*, 2012
- [55] S. Hofmann, M. Cantoro, B. Kleinsorge, C. Casiraghi, A. Parvez, and J. Robertson, “*Effects of catalyst film thickness on plasma-enhanced carbon nanotube growth*”, *Journal of Applied Physics* Vol. 98, No. 3, 034308, 2005